

RESEARCH PAPER

DS-70, a novel and potent α_4 integrin antagonist, is an effective treatment for experimental allergic conjunctivitis in guinea pigs

Correspondence Santi Spampinato, Department of Pharmacy and Biotechnology, University of Bologna, Irnerio 48, Bologna 40126, Italy. E-mail: santi.spampinato@unibo.it

Received 19 December 2017; **Revised** 12 July 2018; **Accepted** 13 July 2018

Samantha Deianira Dattoli^{1,*}, Monica Baiula^{1,*}, Rossella De Marco², Andrea Bedini¹, Michele Anselmi², Luca Gentilucci²  and Santi Spampinato¹ 

¹Department of Pharmacy and Biotechnology, University of Bologna, Bologna, Italy, and ²Department of Chemistry “G. Ciamician”, University of Bologna, Bologna, Italy

*These authors contributed equally to this study.

BACKGROUND AND PURPOSE

Allergic conjunctivitis is an eye inflammation that involves the infiltration of immune cells into the conjunctiva via cell surface-adhesion receptors, such as integrin $\alpha_4\beta_1$. These receptors interact with adhesion molecules expressed on the conjunctival endothelium and may be a target to treat this disease. We synthesized DS-70, a novel α/β -peptidomimetic α_4 integrin antagonist, to prevent the conjunctival infiltration of immune cells and clinical symptoms in a model of allergic conjunctivitis.

EXPERIMENTAL APPROACH

In vitro, DS-70 was pharmacologically characterized using a scintillation proximity procedure to measure its affinity for $\alpha_4\beta_1$ integrin, and its effect on cell adhesion mediated by different integrins was also evaluated. The effects of DS-70 on vascular cell adhesion molecule-1 (VCAM-1)-mediated degranulation of a human mast cell line and an eosinophilic cell line, which both express $\alpha_4\beta_1$, and on VCAM-1-mediated phosphorylation of ERK 1/2 in Jurkat E6.1 cells were investigated. Effects of DS-70 administered in the conjunctival fornix of ovalbumin-sensitized guinea pigs were evaluated.

KEY RESULTS

DS-70 bound to integrin $\alpha_4\beta_1$ with nanomolar affinity, prevented the adhesion of α_4 integrin-expressing cells, antagonized VCAM-1-mediated degranulation of mast cells and eosinophils and ERK 1/2 phosphorylation. Only 20% was degraded after an 8 h incubation with serum. DS-70 dose-dependently reduced the clinical symptoms of allergic conjunctivitis, conjunctival α_4 integrin expression and conjunctival levels of chemokines and cytokines in ovalbumin-sensitized guinea pigs.

CONCLUSIONS AND IMPLICATIONS

These findings highlight the role of α_4 integrin in allergic conjunctivitis and suggest that DS-70 is a potential treatment for this condition.

Abbreviations

δ , chemical shift; 7-AAD, 7-aminoactinomycin D; AMPUMP, 1-(4-(aminomethyl)phenyl)-3-(O-methyl)urea; Boc, tert-butylloxycarbonyl; DCC, *N,N'*-dicyclohexylcarbodiimide; DIPEA, *N,N*-diisopropylethylamine; DMF, dimethylformamide; ESI-MS, electrospray impact MS; Fmoc, fluorenylmethoxycarbonyl; FN, fibronectin; HBTU, 2-(1*H*-benzotriazol-1-yl)-1,1,3,3-tetramethyluronium hexafluorophosphate; HOBT, hydroxybenzotriazole; ICAM-1, intercellular adhesion molecule-1; IHC, immunohistochemical; mAb, monoclonal antibody; MAdCAM-1, mucosal addressin cell adhesion molecule-1; MBP, major basic protein; MPUPA, *o*-methylphenylureaphenylacetyl; PE, phycoerythrin; RP, reverse phase; SPA, scintillation proximity assay; TFA, trifluoroacetic acid; VCAM-1, vascular cell adhesion molecule-1

Introduction

Allergic conjunctivitis includes a variety of ocular inflammatory diseases that are mainly caused by type 1 hypersensitivity reactions related to the preferential generation of IgE antibodies (Baiula and Spampinato, 2014). The early phase reaction occurs when allergens recognize IgE antibodies bound to the high-affinity receptor for the Fc region of IgE on conjunctival mast cells. This event triggers mast cell degranulation, histamine release and the generation of prostaglandins, leukotrienes, cytokines and chemokines, causing ocular itching and hyperaemia. Additional symptoms include swelling of the surrounding eyelids, chemosis and tearing. The early phase reaction leads to a late phase after 6–12 h that is sustained by T-cell-dependent processes through the production of cytokines and chemokines that mediate the recruitment and conjunctival infiltration of eosinophils and other immune cells (Choi and Bielory, 2008). This latter event requires the interaction between leukocyte surface-adhesion receptors, such as **integrins** and selectins, and adhesion molecules expressed on the conjunctival endothelium, such as intercellular adhesion molecule-1 (**ICAM-1**) (Oh *et al.*, 1999) and vascular cell adhesion molecule-1 (**VCAM-1**) (Baiula *et al.*, 2012). Increased levels of cell adhesion molecules on the microvasculature and factors that regulate these molecules may perpetuate inflammation in allergic conjunctivitis (Okada *et al.*, 2005).

Integrin α_4 associates with a β_1 or β_7 subunit on leukocytes to form the integrin heterodimers $\alpha_4\beta_1$ and $\alpha_4\beta_7$ that mediate cell adhesion to VCAM-1 and **fibronectin** (FN) and behave as both adhesion and signalling molecules (Kummer and Ginsberg, 2006). Integrin $\alpha_4\beta_7$ is predominantly expressed in a subpopulation of CD4(+) CD45RA(+) T-cells, which have been shown to preferentially home to the gut through interactions with mucosal addressin cell adhesion molecule-1 (**MAdCAM-1**) (Wright *et al.*, 2002).

Integrin $\alpha_4\beta_1$ is expressed in mast cells, which contributes to the recruitment and influences migration and functional responses (Hallgren and Gurish, 2011). This integrin is also expressed on eosinophils (Barthel *et al.*, 2008), mediating their activation and infiltration in inflamed tissues (Ahmadzai *et al.*, 2015), including the conjunctiva (Abu el-Asrar *et al.*, 1997; Baiula *et al.*, 2012). Studies using monoclonal antibodies have confirmed that α_4 integrin contributes to eosinophil recruitment in allergic inflammatory diseases (Ebihara *et al.*, 1999; Fukushima *et al.*, 2006). Based on these findings, the blockade of $\alpha_4\beta_1$ integrin may represent a useful therapeutic strategy to treat allergic eye diseases. Current therapies for allergic conjunctivitis mainly include antihistamines and mast cell-stabilizing agents that only alleviate clinical symptoms, or glucocorticoids whose use is limited by adverse effects (Abelson *et al.*, 2015). Therefore, safer and more effective drugs are required to treat allergic eye diseases (Baiula and Spampinato, 2014).

Low MW antagonists of integrin α_4 decrease airway inflammation in animal models of allergic asthma (Cortijo *et al.*, 2006; Kenyon *et al.*, 2009). Furthermore, topical administration of an α_4 integrin antagonist improves ocular surface inflammation in a murine model of dry eye (Ecoiffier *et al.*, 2008) and in established ocular surface disease associated with Sjögren's syndrome (Contreras-Ruiz *et al.*, 2016). The

efficacy of α_4 integrin antagonists in treating allergic conjunctivitis has been poorly explored. Drugs are frequently administered topically in the conjunctival fornix to treat this pathology (Baiula and Spampinato, 2014), and low MW α_4 antagonists are suitable for administration via this route.

In the present study, we report the synthesis of two novel hybrid α/β -peptides and their pharmacological characterization as potent and selective α_4 integrin antagonists. Recently, we described a series of $\alpha_4\beta_1$ integrin antagonists based on a β -amino acid central core, an α_4 integrin-targeting diphenylurea moiety and a moiety carrying a β_1 -targeting acidic functionality at the C terminus flanked by an aromatic substituent (Dattoli *et al.*, 2014; De Marco *et al.*, 2015). The β -amino acids were chosen to increase peptide stability and for the conformational control exerted on the overall structure (De Marco *et al.*, 2016). Following these early investigations, we synthesized the novel hybrid α/β -peptidomimetics DS-70 and DS-23, which include a (D)-configured β^2 -proline (the D configuration of this β -residue corresponds to the S absolute stereochemistry). Similar to the reference compound **BIO1211**, DS-70 showed a linear sequence completed by o-methylphenylureaphenylacetyl (MPUPA) and a simple glycine. In contrast, DS-23 represented the partially retro analogue of DS-70, since the β -amino acid central core was connected to 1-(4-(aminomethyl)phenyl)-3-(O-methyl)urea (AMPUMP) and to the diacid equivalent of glycine (Figure 1). Indeed, retro-peptide sequences showed higher efficacy against $\alpha_4\beta_1$ integrins compared to the corresponding normal sequences in our previous studies (Dattoli *et al.*, 2014; De Marco *et al.*, 2015).

Pharmacological characterization of these novel compounds was performed *in vitro* using a scintillation proximity procedure to measure their affinity for $\alpha_4\beta_1$ integrin, and their effects on cell adhesion mediated by this integrin were also evaluated. DS-70 was the most potent compound and was assayed in VCAM-1-mediated degranulation of HMC 1.1 cells, a human mast cell line, and EoL-1 cells, a human eosinophilic leukaemia cell line, both of which express $\alpha_4\beta_1$ integrin (Sperr *et al.*, 1992; Jung *et al.*, 1994). Furthermore, DS-70 antagonized VCAM-1-mediated phosphorylation of **ERK 1/2** in Jurkat E6.1 cells. Finally, the effects of topical treatment with DS-70 on a guinea pig model of allergic conjunctivitis were evaluated. DS-70 dose-dependently reduced clinical aspects of allergic conjunctivitis, conjunctival mast cell and eosinophil infiltration, α_4 integrin expression and levels of mRNAs for IL-1 β , **IL-8 (CXCL8)**, **CCL5** and **CCL11**. Protein levels of these latter chemokines were also measured. To the best of our knowledge, this report is the first to describe a low MW compound that acts as an effective antagonist of α_4 integrin, following direct administration in the conjunctival fornix in a model of allergic conjunctivitis.

Methods

General procedure for the synthesis of peptidomimetics

Standard chemicals and the protected amino acids were obtained from commercial sources and used without any purification. The purity of intermediates and final products were analysed by reverse-phase (RP)-HPLC, performed on Agilent

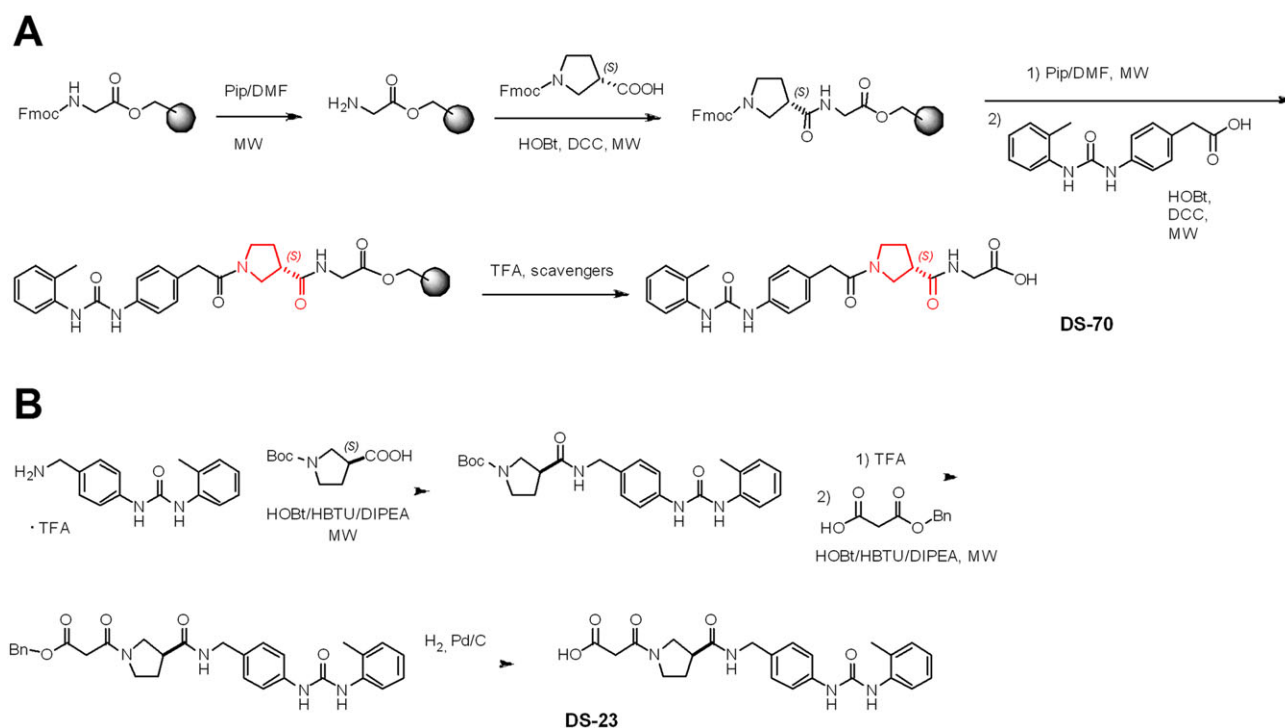


Figure 1

Structures of the N-to-C-terminus 'straight' sequence DS-70 of its partially retro-analogue DS-23 and the well-known $\alpha_4\beta_1$ antagonist BIO1211, showing a first inversion of the sequence between the diphenylurea group and the C-to-N oriented β^2 -Pro and a second inversion between the latter and the malonate.

1100 series apparatus, equipped with a RP column Phenomenex (Torrance, CA, USA) No 00D-4439-YO Gemini 3 μm C18 110 \AA , LC column 100 \times 3.0 mm; diode-array detection was set at 210 nm. Mobile phase description: gradient from 0.1% formic acid (0.1 mL·100 mL⁻¹) in H₂O/acetonitrile (9:1) up to formic acid (0.1 mL·100 mL⁻¹) in H₂O/acetonitrile (2:8) in 20 min, flow rate = 1.0 mL·min⁻¹. Semi-preparative RP-HPLC utilized an Agilent 1100 series apparatus (Agilent, Technologies, Waldbronn, Germany), equipped with a RP column ZORBAX No 977150-102 Eclipse XDB C18 PrepHT cartridge 21.2 \times 150 mm, 7 μm (Agilent Technologies). Mobile phase description: gradient from trifluoroacetic acid (TFA; 0.1 g·100 mL⁻¹) in H₂O/acetonitrile (8:2) to TFA (0.1 mL·100 mL⁻¹) in acetonitrile (100%) in 10 min, flow rate = 12 mL·min⁻¹. Electrospray ionization MS analysis was performed on a HP mass spectrometer MSD 1100 detector (Agilent Technologies) with single quadrupole. The procedures under microwave irradiation utilized the microwave oven Micro-SYNTH microwave labstation (Milestone Inc., Shelton, CT, USA) and temperature was controlled by using a built-in advanced fibre optic automatic control. ¹H NMR analysis was performed on an apparatus Varian Gemini 400 MHz (Agilent Technologies); peptide samples were dissolved in DMSO-*d*₆ to the final concentration of 0.01 M and analysed in 5 mm tubes at room temperature. Solvent suppression of residual moisture required the standard 'PRESAT' solvent presaturation procedure; chemical shifts (δ) are expressed as p.p.m. DMSO was used as an internal standard, by setting $\delta\text{H} = 2.50$ p.p.m. The following abbreviations are used: s, singlet; d, doublet; t, triplet; dd,

double doublet and m, multiplet. The assignment of all resonances was based on two-dimensional gradient selected correlation spectroscopy experiments.

Synthesis of DS-70

Fmoc (fluorenylmethoxycarbonyl)-Gly-Wang preloaded resin (Sigma-Aldrich, Milan, Italy; 0.5 g, amino acid load = 0.4–0.8 mmol·g⁻¹ according to the manufacturer) was placed into a syringe equipped with a frit.

Fmoc deprotection. The Fmoc protecting group was cleaved in 2 min by treatment with 20% piperidine in dimethylformamide (DMF) (5 mL) while bubbling nitrogen, under microwave irradiation (irradiation power = 40 W, internal reaction temperature = 45°C; see above). The resin was filtered and washed with CH₃OH (5 mL), DMF (5 mL) and CH₂Cl₂ (5 mL) in sequence. The cleavage procedure and washes were repeated twice as described above. The deprotection was qualitatively assessed by a positive Kaiser test.

Coupling. The acid-partner (0.9 mmol) was dissolved in DMF (6 mL) at room temperature, in the presence of hydroxybenzotriazole (HOBt) (0.9 mmol) and *N,N'*-dicyclohexylcarbodiimide (DCC) (0.9 mmol). After stirring for 5 min, the mixture was added to the resin pre-swollen in CH₂Cl₂ (5 mL). The suspension was mechanically shaken for 10 min under microwave irradiation. Then, the resin was filtered and washed three times with the same solvents as described in the paragraph above. The coupling was assessed by the Kaiser test. The repetitive deprotection and

coupling steps were carried out according to the same protocols and workup procedures (Figure S1A).

Peptide cleavage. The peptidyl-resin obtained according to the previous protocol was pre-swollen in CH_2Cl_2 (3 mL) and treated with a 90:5:5 mixture of TFA/ H_2O /triisopropylsilylether (10 mL), plus phenol (50 mg), and the mixture was mechanically shaken at room temperature for 2 h. Subsequently, the cocktail was filtered to recover the peptide, and the unloaded resin was washed with 20% TFA in diethyl ether (5 mL), CH_2Cl_2 (5 mL) and CH_3OH (5 mL) in sequence. The filtrates were collected; the volatiles were removed with a moderate nitrogen flow at room temperature. The solid residue was suspended in ice-cold diethyl ether to favour peptide precipitation. The crude peptide was triturated and collected by centrifugation at $2000\times g$ for 10 min.

The peptide was isolated (78% yield) by semipreparative RP-HPLC, and purity was assessed by analytical RP-HPLC (98%). The correct compositions were determined by electrospray impact MS (ESI-MS) analyses. DS-70 was analysed by ^1H NMR spectroscopy. ^1H NMR (3:1 deuterated chloroform/DMSO- d_6 , 400 MHz) δ (the spectrum shows two sets of signals in 1:1 ratio, relative to conformers A and B around the amide bond which precedes β -Pro): 1.82–2.03 (m, $2\text{H}_{\text{A+B}}$, β -ProH $_{\text{A+B}}$), 2.05 (s, $3\text{H}_{\text{A+B}}$, $\text{Me}_{\text{A+B}}$), 2.78 (m, 1H_{A} , β -ProH $_{3\text{A}}$), 2.86 (m, 1H_{B} , β -ProH $_{3\text{B}}$), 3.16 (m, 1H_{B} , β -ProH $_{5\text{B}}$), 3.24 (m, 1H_{A} , β -ProH $_{5\text{A}}$), 3.33–3.39 (m, 2H_{A} , β -ProH $_{2\text{A}}$ + β -ProH $_{5\text{A}}$), 3.39–3.49 (m, $2\text{H}_{\text{A+B}}$ + 3H_{B} , $2\times\text{CH}_2\text{CO}_{\text{A+B}}$ + $1\times\beta$ -ProH $_{5\text{B}}$ + $2\times\beta$ -ProH $_{2\text{B}}$), 3.54 (dd, $J = 8.0, 13.6$ Hz, 1H_{A} , β -ProH $_{2\text{A}}$), 3.70 (d, $J = 4.8$ Hz, $2\text{H}_{\text{A+B}}$, GlyH $\alpha_{\text{A+B}}$), 6.73 (t, $J = 7.2$ Hz, $1\text{H}_{\text{A+B}}$, ArH $_{4'\text{A+B}}$), 6.83–6.97 (m, $4\text{H}_{\text{A+B}}$, ArH $_{3'\text{A+B}}$ + ArH $_{5'\text{A+B}}$ + ArH $_{2\text{A+B}}$), 7.19 (d, $J = 7.6$ Hz, $2\text{H}_{\text{A+B}}$, ArH $_{3\text{A+B}}$), 7.22 (s, $1\text{H}_{\text{A+B}}$, ureaNH $_{\text{A+B}}$), 7.62 (d, $J = 8.0$ Hz, $1\text{H}_{\text{A+B}}$, ArH $_{6'\text{A+B}}$), 8.37 (s, $1\text{H}_{\text{A+B}}$, ureaNH $_{\text{A+B}}$), 9.20 (br.s, $1\text{H}_{\text{A+B}}$, COOH $_{\text{A+B}}$). MS m/z [$M + 1$] calculated for $\text{C}_{23}\text{H}_{26}\text{N}_4\text{O}_5$: 439.19; found: 439.30.

BIO1211 (*N*-[[[4-[[[2-methylphenyl]amino]carbonyl]amino]phenyl]acetyl]-*L*-leucyl-*L*-aspartyl-*L*-valyl-*L*-proline) (Figure 1) was prepared adopting the above-described procedure. Purity evaluated by analytical RP-HPLC was 98%. MS m/z [$M + 1$] calculated for $\text{C}_{36}\text{H}_{48}\text{N}_6\text{O}_6$: 709.35; found: 709.40.

Synthesis of DS-23

Boc (tert-butyloxycarbonyl)- β -Pro (1.0 mmol) was dissolved in 4:1 CH_2Cl_2 (5 mL) in the presence of HOBt (1.1 mmol) and 2-(1*H*-benzotriazol-1-yl)-1,1,3,3-tetramethyluronium hexafluorophosphate (HBTU; 1.1 mmol), and the mixture was stirred at room temperature under an inert atmosphere for 5 min. Thereafter, AMPUMP-TFA salt (1.1 mmol) was added at room temperature while stirring, followed by *N,N*-diisopropylethylamine (DIPEA; 2.2 mmol). The mixture was stirred for 10 min under microwave irradiation (see above). The mixture was diluted with CH_2Cl_2 (40 mL) and washed with 0.5 M HCl (5 mL) and with saturated solution of NaHCO_3 (5 mL). The organic layer was dried over Na_2SO_4 , and solvent was removed at reduced pressure. The protected intermediate was isolated (75%) by flash chromatography over silica-gel (eluent: 100% ethyl acetate).

Subsequently, the Boc group was removed by treatment with 25% TFA in CH_2Cl_2 (10 mL). The mixture was subjected to moderate nitrogen flow at room temperature until a solid residue was obtained.

The resulting TFA salt was utilized without purification and coupled with 3-(benzyloxy)-3-oxopropanoic acid under the same conditions as described above, following the same work up, including the isolation of the intermediate.

The benzyl ester was removed by treatment with H₂ palladium on carbon in ethanol for 4 h (Figure S1B) at room temperature. The mixture was filtered over Celite® (Sigma-Aldrich), and the filter was washed with ethanol (10 mL). After evaporation of the collected ethanol layers at reduced pressure, the final purification of the residue was accomplished with semi preparative RP-HPLC, and purity was determined by analytical RP-HPLC (97%; see the General procedure for the synthesis of peptidomimetics). MS m/z [$M + 1$] 439.2; calculated for $\text{C}_{23}\text{H}_{26}\text{N}_4\text{O}_5$: 439.19; found: 439.20.

Animals

All animal care and experimental protocols complied with the EU Directive 2010/63 and the D. Lgs. 116/92 of the Italian legislation in effect at the time of the study (June and July, 2012). The Scientific Ethics Committee on Animal Experimentation of the University of Bologna approved the experimental protocol adopted (protocol n. 31331-X/10; July 22, 2011). This study followed the editorial on experimental design and analysis in pharmacology (Curtis *et al.*, 2018). Animal studies are reported in compliance with the ARRIVE guidelines (Kilkenny *et al.*, 2010; McGrath & Lilley, 2015). Fifty male Hartley albino guinea pigs (250–300 g, 6- to 8-week-old) obtained from Charles River Laboratories Italia (Calco, Italy) were used. Animals were housed in groups of five to six in a controlled environment at 22–24°C and humidity 60–62%, with a 12 h light/dark cycle and access to food (Teklad Global Guinea Pig Diet 2040) and tap water *ad libitum*. All efforts were made to minimize animal suffering. The cages contained soft bedding and environmental enrichment for welfare purposes, and the animals were allowed to acclimatise to this environment for 7–9 days after arrival in the unit before use.

Ovalbumin sensitization

Animals were sensitized to chicken-derived ovalbumin using aluminium hydroxide as an adjuvant to promote an IgE-mediated conjunctival allergic response (Groneberg *et al.*, 2003). Guinea pigs were randomly divided into eight experimental groups of five animals per group. Group sizes were based on our earlier studies with the ovalbumin-challenge model showing a significant and reproducible conjunctival inflammation with eosinophil infiltration (Qasem *et al.*, 2008; Baiula *et al.*, 2011). Five groups were sensitized on days 1, 7 and 14 by an i.p. injection of 200 μg of ovalbumin with 40 mg of aluminium hydroxide suspended in 200 μL of saline, as previously reported (Qasem *et al.*, 2008), and three groups received an i.p. injection of 200 μL of saline (control). On day 21, sensitized guinea pigs and one control group received 30 μL of saline containing 3 mg of ovalbumin in the conjunctival fornix of both eyes; 30 and 10 min before ovalbumin challenge, three groups of sensitized animals

received 30 μL of a vehicle containing 0.01, 0.05 and 0.1%, (w/v) of DS-70, respectively, in the conjunctival fornix of both eyes and gently closing the eyelid to prolong the drug residence time in the conjunctiva (Awwad *et al.*, 2017). Another group of ovalbumin-sensitized guinea pigs and a control group received 30 μL of vehicle per eye 30 and 10 min before ovalbumin challenge. The second control group received 30 μL of 0.1 g·100 mL⁻¹ DS-70 in both eyes 30 and 10 min before topical saline administration. The last control group received dexamethasone (30 μL of 0.1 g·100 mL⁻¹; 0.1%), 30 and 10 min before topical saline administration. Finally, an ovalbumin-sensitized guinea pig group received 30 μL of 0.1% dexamethasone in both eyes 30 and 10 min before ovalbumin challenge.

Clinical conjunctival symptoms were rated in both eyes using the following scale: 0, no symptoms; 1, slight conjunctival redness with or without tears; 2, mild conjunctival redness with or without tears and mild chemosis; 3, mild conjunctival redness with or without tears and moderate chemosis; 4, severe conjunctival redness with tears and partial lid eversion; 5, severe conjunctival redness with tears and lids more than half closed. Photographs of both eyes were taken to evaluate the clinical score 30 min before ocular treatments and 1, 2, 4, 6 and 24 h after ovalbumin administration. The animals were killed 24 h after ovalbumin challenge. Guinea pigs were sedated, prior to ovalbumin challenge, with a mixture of Ketalar® and Rompun® (32 mg·kg⁻¹ Ketalar and 2.3 mg·kg⁻¹ Rompun), given i.p.. The animals were killed 24 h later with 100 mg·kg⁻¹ of pentobarbital, i.p..

Tarsal conjunctiva were carefully excised from both eyes and divided into separate samples for subsequent investigations. One sample was fixed with a 10% buffered paraformaldehyde solution and embedded in paraffin. Slices (6 μm thick) were stained to determine the number of mast cells and eosinophils and to perform immunohistochemical (IHC) assays. Other samples were collected to quantify eosinophil peroxidase activity, cytokine and chemokine mRNA levels.

Conjunctival absorption of DS-70

To evaluate the conjunctival absorption of DS-70 in guinea pigs, this compound (30 μL of 0.1 g·100 mL⁻¹) was administered in the right eye, whereas the contralateral eye was treated with the vehicle used to dissolve DS-70. Two treatments were given, 30 min apart. Guinea pigs (five per group) were killed with pentobarbital (100 mg·kg⁻¹ i.p.), 1 h or 6 h after the first treatment. Tarsal conjunctiva was collected, weighed and processed as described (Iyer *et al.*, 2015) to extract DS-70. Internal standard was **levocabastine** hydrochloride (0.5 mg·mL⁻¹). DS-70 was quantified using a standard curve (84 $\mu\text{g}\cdot\text{mL}^{-1}$ –27 ng·mL⁻¹). Detection of DS-70 and levocabastine was carried out as previously described in the paragraph 'Synthesis of DS-70'.

Validity of animal species and model selected for study

Allergic conjunctivitis is a localized pathological condition that is observed as the only or dominant presentation of an allergic sensitization when an allergen irritates conjunctiva or is associated with rhinitis. Ocular symptoms, which are estimated to be present in more than 75% of allergic patients,

include itching, tearing, redness and swelling, but no pain. Signs and symptoms of allergic conjunctivitis involve a complex series of immunological mechanisms initiated by the sensitization to a novel allergen. Upon re-exposure, the antigen is recognized by allergen-specific IgE receptors located on conjunctival mast cells, leading to their activation and degranulation (Baiula and Spampinato, 2014). We have adopted a guinea pig model of allergen exposure and challenge (Qasem *et al.*, 2008; Baiula *et al.*, 2014) that is similar to models used in the clinic.

Conjunctival manifestations of ocular allergy are caused by immune cell activation and the release of allergic mediators on the ocular surface that have been detected in animal models and in patients (Groneberg *et al.*, 2003). Several inflammatory intermediates, such as proteins, cytokines and chemokines, have been proposed as potential biomarkers of allergic conjunctivitis in patients (Irkec and Bozkurt, 2012) and have been assayed in animal models (Baiula *et al.*, 2014). In contrast to the large amount of experimental studies on allergic asthma, few experimental studies have used models of allergic eye diseases. Guinea pigs are among the major laboratory animal species employed for the assessment of ocular allergies, as they have proved to be a valid model to assess the anti-allergic effects of established and newly developed compounds, which are mainly administered directly into the conjunctival sac (Groneberg *et al.*, 2003).

Cell culture

All cell lines were purchased from the ATCC (Rockville, MD, USA) except as otherwise specified. Cell culture medium of each cell line is described in detail in Table S2. HEL cells were a kind gift from C. Prata and L. Zamboni (Mayo Foundation for Medical Education and Research, Rochester, MN, USA); MCF7 and HT-29 cells were a kind gift from Prof. N. Calonghi (Mayo Foundation for Medical Education and Research, Rochester, MN, USA). D283 cells were kindly donated by Prof. G. Cenacchi (Mayo Foundation for Medical Education and Research, Rochester, MN, USA). RPMI 8866 cells were a kind gift from Prof. A. Santoni (Mayo Foundation for Medical Education and Research, Rochester, MN, USA); this cell line were usually kept in 50 mL of culture medium and allowed to form large clumps. HMC 1.1 cells were kindly provided by Prof. J. H. Butterfield (Mayo Foundation for Medical Education and Research, Rochester, MN, USA). Cells were kept at 37°C under 5% CO₂ humidified atmosphere. As regards K562 and HL60 cells, 40 h in advance of the adhesion assays, they were treated with phorbol 12-myristate 13-acetate (Sigma-Aldrich) in a concentration of 25 and 40 ng·mL⁻¹ respectively. This treatment induced cell differentiation and increased expression of $\alpha_5\beta_1$ and $\alpha_M\beta_2$ integrins on the cell surface (Baiula *et al.*, 2016). Integrin expression in the cell lines noted above has been previously described (Erle *et al.*, 1994; Baiula *et al.*, 2016) and is summarized in Table S2.

Scintillation proximity assay

We modified a scintillation proximity assay (SPA) previously developed in our laboratory (Qasem *et al.*, 2008) to detect competitive binding of the tested compound to soluble [¹²⁵I]-human FN (MW approximately 440 kDa) bound to an antibody-captured integrin $\alpha_4\beta_1$ complex. $\alpha_4\beta_1$ integrin was extracted from Jurkat E6.1 cells and purified by affinity

chromatography, following a procedure to extract membrane proteins (Qasem *et al.*, 2008). The experiments were carried out in scintillation vials kept in the dark; an aliquot of cell eluate containing approximately 100 µg of $\alpha_4\beta_1$ integrin was added together with increasing concentrations of the tested compounds for 90 min at room temperature. Then, the rabbit anti-human α_4 integrin antibody was added for 1 h at 4°C. Thereafter, the beads coated with the anti-rabbit IgG antibody (400 ng) were added, and the mixture was incubated for 2 h at 4°C. Finally, we added [125 I]-FN (10^5 counts per minute) to the vials that were then incubated for 24 h at room temperature on a shaker. Non-specific binding was determined in the presence of the specific $\alpha_4\beta_1$ integrin antagonist BIO1211 (100 mM). Bead-associated radioactivity was measured using a LS 6500 multipurpose scintillation counter (Beckham Coulter, Fullerton, CA, USA). The concentration of the compounds causing 50% inhibition of binding of [125 I]-human FN to $\alpha_4\beta_1$ integrin was calculated (IC₅₀).

Cell adhesion assays

The assays were performed as previously described (Tolomelli *et al.*, 2015; Baiula *et al.*, 2016). SK-MEL-24, K562, D283 and HT-29 cells were seeded in 96-well plates coated by passive adsorption with FN (10 µg·mL⁻¹) overnight at 4°C. For MCF7, HEL and HL60 cells, the plates were coated with **fibrinogen** (10 µg·mL⁻¹). In adhesion assays carried out with Jurkat E6.1, EoL-1 and HMC 1.1 cells, plates were coated with VCAM-1 (2 µg·mL⁻¹) or FN (10 µg·mL⁻¹). Alternatively, Jurkat E6.1 cell adhesion assays were performed in plates coated with ICAM-1 (2 µg·mL⁻¹). A saturation curve for each ligand was plotted to establish the best signal-to-noise ratio. Non-specific hydrophobic binding sites were blocked, for 30 min at 37°C, by incubation with BSA (1 g·100 mL⁻¹) dissolved in HBSS.

The number of adherent cells was calculated by comparison with a standard curve prepared in the same plate using known concentrations of labelled cells. The effect of antagonists was evaluated by the reduction in adherent cells in comparison to the controls. Adhesion assays were also carried out in the presence of an anti-human α_4 integrin antibody (5 µg·mL⁻¹). Experiments were carried out in quadruplicate and repeated at least five times.

Western blot analysis

Jurkat E6.1, EoL-1 and HMC 1.1 cells were cultured for 16/18 h in medium containing a reduced amount of FBS (1 g·100 mL⁻¹). Then, 3×10^6 cells were pre-incubated with different concentrations of DS-70 for 60 min and then seeded for 1 h in VCAM-1-(2 µg·mL⁻¹) coated plates and lysed on ice using a mammalian protein extraction reagent (M-PER; Pierce, Rockford, IL, USA) in the presence of a phosphatase inhibitor cocktail. Protein extracts were quantified using a BCA protein assay kit (Pierce, Rockford, IL, USA), heated for 5 min at 95°C, and equal amounts of the samples were separated by 12% SDS-PAGE gel, transferred onto nitrocellulose membranes and immunoblotted with the indicated antibodies. Incubations with anti-phospho-ERK 1/2 (1:1000) (Cell Signaling Technology, Danvers, MA, USA) or anti-total ERK1/2 antibodies (1:2500) (Cell Signaling Technology) took place overnight at 4°C in the presence of BSA (5 g·100 mL⁻¹) in Tris buffered-saline containing Tween-20 (0.1 g·100 mL⁻¹). After washing, anti-rabbit HRP-conjugated secondary

antibodies (Santa Cruz Biotechnology, Dallas, TX, USA) were added to membranes for 1.5 h at room temperature. Protocols for image acquisition and analysis have been previously described (Bedini *et al.*, 2008).

HUTS-21 monoclonal antibody binding

Flow cytometry analysis was carried out in accordance to protocols previously described (Baiula *et al.*, 2016). Jurkat E6.1 cells were suspended in BSA/HBSS (10⁶ cells·mL⁻¹; 100 µL per sample) and kept at 37°C. Then, VCAM-1 (2 µg·mL⁻¹) and different concentrations of DS-70 (10⁻⁴–10⁻¹⁰ M) were added to the cells for 30 min. Thereafter, phycoerythrin (PE)-conjugated HUTS-21 monoclonal antibody (mAb) (PE mouse anti-human CD29 antibody, Becton Dickinson Italia, Milan, Italy) (20 µL per sample) was added for 45 min at room temperature to assure an optimal labelling. After two washes with BSA/HBSS, the cells were suspended in PBS, and 10 000 cells per sample were analysed in a Guava[®] EasyCyte Flow Cytometer (Merck, Milan, Italy). The data are presented as mean channel fluorescence, at each concentration of DS-70. Control cells were exposed to an isotype control mAb (PE mouse IgG2a, k isotype control clone G155-178, Becton Dickinson Italia), and the measured fluorescence intensity was considered as non-specific binding and subtracted from total fluorescence.

Flow cytometry

For the detection of cell surface α_4 integrin, cells were collected from culture plates, washed two times with PBS and incubated with a FITC-labelled anti- α_4 antibody (FITC Mouse anti-human CD49d, Becton Dickinson Italia) (5 µL per sample) for 45 min at room temperature. Flow cytometry was performed using a Guava EasyCyte Flow Cytometer (Merck).

To detect any apoptosis and/or necrosis in Jurkat E6.1, EoL-1 and HMC 1.1 cell lines exposed to DS-70, 75 000 cells per well were incubated with the compound (10⁻⁴ M) for 6 h at 37°C. A mixture 1:1 of complete medium/Guava Nexin Reagent (Merck) was added to cells, following the manufacturer's instructions for staining. Viable cells [annexin V-PE and 7-aminoactinomycin D (7-AAD) negative], early apoptotic cells (annexin V-PE positive and 7-AAD negative), and late stage apoptosis or necrotic cells (annexin V-PE and 7-AAD positive) were separately counted. At least 10.000 cells per sample were acquired.

Cell degranulation assays

Degranulation assays were carried out in HMC 1.1 and EoL-1 cells. β -Hexosaminidase, a marker of mast cell degranulation, was quantitated to measure HMC 1.1 degranulation as these cells exhibit many characteristics of tissue mast cells (Sundström *et al.*, 2003). Each experiment was carried out in triplicate and repeated at least five times. Values are expressed as percentage of degranulation and derived from the following equation: (experimental β -hexosaminidase release – vehicle β -hexosaminidase release)/(Triton X-100 β -hexosaminidase release – vehicle control β -hexosaminidase release) \times 100.

The *o*-phenylenediamine method previously described by us (Qasem *et al.*, 2008) was used to measure eosinophil peroxidase release. Measurement of absorbance was performed at 490 nm using a Victor² multilabel counter (PerkinElmer, Milan, Italy). Each experiment was carried out in triplicate and repeated at least five times.

Histological and immunofluorescent detection of mast cells and eosinophils

Degranulated mast cells were evaluated in photographs of three random sections (6 μm thick) per eye obtained from tarsal conjunctiva specimens, stained in May–Grünwald–Giemsa solution (Sigma-Aldrich) for 60 min at room temperature and detected with a light microscope Nikon Eclipse E800 (Nikon Instruments S.p.a., Florence, Italy) (400 \times magnification).

Histological sections of tarsal conjunctiva (6 μm thick) were processed to determine eosinophil infiltration using a classical Luna's protocol (Baiula *et al.*, 2011). The sections were immersed in haematoxylin-Biebrich scarlet solution for 5 min, dipped ($\sim 8\times$) in 1% acid alcohol (Sigma-Aldrich) and rinsed in water. Sections were then dipped ($\sim 5\times$) in lithium carbonate (0.5 g \cdot 100 mL $^{-1}$) until turned blue and washed in running tap water. Pictures were taken of three random sections per eye, and eosinophils were detected under light microscopy (500 \times magnification). Eosinophils or degranulated mast cells were counted and expressed as number of cells \cdot mm $^{-2}$.

For co-labelling experiments, conjunctival sections were incubated with blocking solution containing BSA (1 g \cdot 100 mL $^{-1}$), glycine (22.5 mg \cdot mL $^{-1}$) and Tween20 (0.1 g \cdot 100 mL $^{-1}$) in PBS for 30 min. Then, tissues were incubated with primary antibody overnight at 4°C in a humidified chamber; primary antibody included: rabbit polyclonal anti-integrin α_4 antibody (diluted 1:100; Abcam, Cambridge, UK), mouse anti-human mast cell tryptase antibody (clone AA1, diluted 1:200; BioRad, Milan, Italy) and mouse anti-human eosinophil major basic protein (MBP) antibody (clone BMK13, diluted 1:200, EMD Millipore, Merck S.p.a., Milan, Italy). Conjunctival sections were simultaneously labelled with mixtures of α_4 integrin antibody with either anti-tryptase or anti-MBP antibody. After three washes in PBS, tissues were incubated with a mixture of secondary antibodies: goat anti-mouse antibody labelled with AlexaFluor 488 and goat anti-rabbit antibody labelled with AlexaFluor 568, both diluted 1:500. Digital images were captured using a Nikon C1s (Nikon Instruments S.p.a., Florence, Italy) confocal laser-scanning microscope. Anti-human mast cell tryptase and anti-human MBP antibodies have already been employed to label guinea pigs tissues.

Eosinophil peroxidase assay

In separate conjunctival specimens, eosinophil peroxidase activity was assayed as previously described (Qasem *et al.*, 2008). The tissues were homogenized with 50 mmol \cdot L $^{-1}$ Tris–HCl buffer (pH 8.0) on ice, and after adding 50 mmol \cdot L $^{-1}$ Tris–HCl buffer and 0.1% Triton X-100, homogenates were placed in an ice bath for 1 h. Then, the substrate solution (50 mmol \cdot L $^{-1}$ Tris–HCl buffer containing 0.1% Triton X-100, 1 mmol \cdot L $^{-1}$ *o*-phenylenediamine, 3 mmol \cdot L $^{-1}$ KBr and 0.5 mmol \cdot L $^{-1}$ hydrogen peroxide) was added to samples and incubated at 37°C for 10 min. The reaction was stopped with 4 mol \cdot L $^{-1}$ H $_2$ SO $_4$. Absorbance was measured using a spectrophotometer at 490 nm. The oxidation of *o*-phenylenediamine, in the presence of hydrogen peroxide and KBr, was used to measure the peroxidase-mediated catabolism of hydrogen peroxide. One unit corresponds to 1 mmol of hydrogen peroxide decomposed in 10 min. Results are expressed as mU of enzyme \cdot mg $^{-1}$ wet tissue.

IHC analysis

Slices prepared from tarsal conjunctiva specimens were subjected to deparaffination in xylene and rehydration in serial dilutions of ethanol. Antigen retrieval step was done in citrate buffer (pH 6.0) for 20 min. Sections were washed three times in Tris-buffered saline containing Tween-20 (0.025 g \cdot 100 mL $^{-1}$) (Sigma-Aldrich).

Complete staining was achieved by means of a specific HRP/DAB detection kit (Abcam). The reagents constitute a labelled streptavidin-biotin immuno-enzymic antigen detection system. Briefly, after slice incubation with a protein blocking buffer (Abcam), sections were incubated overnight at 4°C with primary antibodies (100 μL per sample) for CCL11 or CCL5 (Abcam; diluted 1:250) or α_4 integrin (Becton Dickinson; diluted 1:500). Slices were incubated with biotinylated goat anti-rabbit IgG to detect CCL5 and CCL11 or goat anti-mouse IgG1 to detect α_4 integrin for 10 min at room temperature and were developed according to the manufacturer's instructions. Isotype negative controls were performed with an isotype-matched antibody. A mouse IgG1 (Abcam) was the negative control for integrin α_4 and a rabbit IgG polyclonal antibody (Abcam) the negative control for CCL5 and CCL11. Anti-human antibodies for CCL5, CCL11 and α_4 integrin were employed as their protein sequences are almost completely conserved between human and guinea pig and other researchers have previously employed those antibodies in guinea pig tissues successfully.

Relevant photomicrographs were taken with a 20 \times objective. The analysis was done on the basis of a validated semiquantitative scoring method (Walker, 2006). The resulting percentage of tissue showing positive staining is expressed as IHC score that was assigned by two blinded researchers to quantitate IHC-positively stained cells and areas, according to five categories: 0, no staining; 1, <25% staining; 2, 25–50% staining; 3, 50–75% staining; and 4, >75% staining.

Real time RT-PCR

Total RNA from tarsal conjunctiva specimens was extracted employing TRI-Reagent. RNase-free DNase treatment was performed for each sample, and 1 μg of RNA was converted into cDNA using the High-Capacity cDNA Reverse Transcription Kit (Life Technologies Italia, Milan, Italy), according to the manufacturer's instructions. GoTaq $^{\text{®}}$ qPCR Master Mix was chosen to perform the reaction as follow: denaturation at 95°C for 10 min, followed by 40 cycles of 95°C denaturation (20 s) and 58°C annealing (1 min). No-template controls and DNA melting curve analysis were used as controls. For data analysis, the threshold cycle (Ct) values were normalized both on the basis of GAPDH content and on the values derived from non-immunized guinea pigs. GAPDH, IL-8, IL-1 β , CCL11 and CCL5 primer sequences are listed in Table S1 and was first reported in Baiula *et al.* (2014).

Data and statistical analysis

All *in vitro* data are the means \pm SD, of at least five independent experiments, whereas for the *in vivo* experiments, five animals per group were included and both eyes were analysed ($n = 10$). Statistical comparisons were performed using one-way ANOVA and *post hoc* Newman–Keuls test. The scores

assigned to the conjunctival symptoms were non-parametrically analysed using the Friedman test, followed by Dunn's *post hoc* comparison. Significant differences among IHC scores were assessed by the Kruskal–Wallis test followed by Dunn's *post hoc* comparison. Data analysis and IC₅₀ values referring to experiments not mentioned above were obtained using GraphPad Prism software (version 5.0; GraphPad Software, Inc., La Jolla, CA, USA). The data deriving from HUTS-21 binding antibody were fitted using the sigmoidal dose–response equation using GraphPad Prism. $P < 0.05$ was considered significant.

Data related to the clinical conjunctival symptoms are presented as scatter plot. As regards the data presented as bar charts, scatter plot analysis did not reveal any unusual or interesting aspect not obvious from the bar chart (George *et al.*, 2017). The data and statistical analysis comply with the recommendations on experimental design and analysis in pharmacology (Curtis *et al.*, 2018).

Blinding procedures in experiments

Researchers involved in the experiments, data collectors, outcome adjudicators and data analysts who did not participate in the study were blinded to reduce the risk of bias. Personnel who did not perform the experiments prepared the compounds administered.

Materials

DS-70 was dissolved in a vehicle containing PEG 3350 (10 g·100 mL⁻¹) and polysorbate 80 (1 g·100 mL⁻¹) in phosphate buffer (pH 7.0). Polyacrylamide gel, ammonium persulfate, sodium dodecyl sulfate, Tween 20, lectin from *Triticum vulgare*, human FN, BSA, 4-nitrophenyl-*N*-acetyl- β -D-glucosaminide, ovalbumin grade V, aluminium hydroxide gel, *o*-phenylenediamine, hydrogen peroxide 30%, Triton-X-100, peroxidase acidic isoenzyme from horseradish, RNAlater, TRI Reagent, Phosphatase Inhibitor Cocktail 3, levocabastine hydrochloride, pentobarbital sodium salt and citrate buffer solution (0.09 M) were obtained from Sigma-Aldrich. Cell culture media, PBS, FBS, HBSS, 5-chloromethylfluorescein diacetate, RNase-free DNase and High-Capacity cDNA Reverse Transcription Kit were from Thermo Fisher Scientific. M-PER was from Pierce. GoTaq qPCR Master Mix was obtained from Promega Corporation (Madison, WI, USA). Soluble human VCAM-1, MAdCAM-1, ICAM-1 and IL-5 were purchased from R&D Systems (Minneapolis, MN, USA). Fibrinogen (plasminogen-depleted from human plasma), mouse anti-human mAb against β_1 subunit was obtained from Merck. Rabbit anti-human mAb against α_4 subunit was purchased from Santa Cruz Biotechnology as well as secondary antibodies for western blot analysis (Santa Cruz, CA, USA). Hybond-ECL nitrocellulose membrane was from GE Healthcare (Chicago, USA). Black and white 96-well clear-bottom plates were purchased from Corning Costar (Celbio, Milan, Italy), and the other plastic disposables were from Sarstedt (Nümbrecht, Germany). All the other reagents were of analytical grade or the highest purity available, purchased from Sigma-Aldrich. Rompun was from Bayer (Milan, Italy) and Ketalar was from Parke Davis (Milan, Italy).

Nomenclature of targets and ligands

Key protein targets and ligands in this article are hyperlinked to corresponding entries in <http://www.guidetopharmacology.org>, the common portal for data from the IUPHAR/BPS Guide to PHARMACOLOGY (Harding *et al.*, 2018), and are permanently archived in the Concise Guide to PHARMACOLOGY 2017/18 (Alexander *et al.*, 2015, 2017).

Results

Peptide synthesis, general procedure

The linear peptides BIO1211 and DS-70 were prepared by solid phase peptide synthesis on a Wang resin, using Fmoc-protected amino acids, under microwave irradiation conditions optimized by us (Gentilucci *et al.*, 2016). The removal of Fmoc group was performed by treatment with piperidine in DMF, under microwave irradiation for 2 min. Coupling between each residue was carried out with the activating agents DCC and HOBT in 4:1 CH₂Cl₂ (dichloromethane)/DMF under microwave irradiation for 10 min. Peptide cleavage was accomplished by treatment of the peptidyl-resin with TFA in CH₂Cl₂ and scavengers. The crude products were simply precipitated from ice-cold diethyl ether and collected in almost quantitative yield by centrifugation.

On the other hand, the retro sequence DS-23 was prepared in solution. AMPUMP was coupled with Boc-protected β -Pro in solution under microwave irradiation, with the aid of HOBT/HBTU/DIPEA. Boc deprotection of the resulting dipeptide was done in TFA and was followed by coupling with 3-(benzyloxy)-3-oxopropanoic acid under the same conditions previously described. The resulting benzyl ester was deprotected by catalytic hydrogenation, giving DS-23 in good yield. Finally, all peptides were purified (96–98%) with semi-preparative RP-HPLC and identified by ESI-MS HPLC.

Binding affinity of α/β -peptides for human $\alpha_4\beta_1$ integrin as measured by SPA and inhibition of α_4 integrin-mediated cell adhesion

The binding of the reference compound BIO1211 and the novel hybrid α/β -peptides to $\alpha_4\beta_1$ integrin was measured using a SPA. [¹²⁵I]-FN was the specific radioligand, and $\alpha_4\beta_1$ integrin was extracted from human Jurkat E6.1 cells (endogenous expression). Western blot analyses of the $\alpha_4\beta_1$ integrin extracted from cell lysates and purified by affinity chromatography confirmed that both α_4 and β_1 integrin subunits are present in the eluate employed in the assay (Figure S2, panel A).

[¹²⁵I]-FN binding was inhibited by the well-established $\alpha_4\beta_1$ integrin antagonist BIO1211 and by the novel hybrid α/β -peptides DS-70 and DS-23 in a concentration-dependent manner. As reported in Table 1, the most effective ligands were DS-70 and BIO1211, which showed the lowest and superimposable IC₅₀ values.

Subsequently, we assayed the ability of hybrid α/β -peptides to inhibit adhesion of $\alpha_4\beta_1$ integrin-expressing Jurkat E6.1 cells to VCAM-1 or FN. Jurkat E6.1 cell adhesion to both adhesion molecules was inhibited (>95%) after treatment with a specific anti- α_4 antibody (data not shown). The

Table 1

SPA binding to bead-associated $\alpha_4\beta_1$ integrin and inhibition of Jurkat E6.1 cell adhesion of the reference compound BIO1211 and hybrid α/β -peptides^a to VCAM-1 ($2 \mu\text{g}\cdot\text{mL}^{-1}$) or FN ($10 \mu\text{g}\cdot\text{mL}^{-1}$).

Compound	SPA IC ₅₀ (nM) ^b	Cell adhesion Jurkat/ VCAM-1 IC ₅₀ (nM)	Cell adhesion Jurkat/ FN IC ₅₀ (nM)
BIO1211	8.80 ± 3.4 (0.08–46.7) ^c	4.60 ± 3.0 (0.05–25.1)	5.50 ± 4.0 (0.09–37.6)
DS-70	8.3 ± 3.2 (0.1–37.2)	5.04 ± 0.51 (0.05–37.3)	4.3 ± 1.7 (0.04–23.4)
DS-23	47.7 ± 4.1 (4.6–161.4)	40.3 ± 7.1 (3.4–127.6)	51 ± 5.0 (4.8–192.4)

^aResults were generated by measuring, in a cell-free SPA, the inhibition of [¹²⁵I]-FN binding by the assayed compounds on Jurkat E6.1 cell lysates in the presence of 10 increasing concentrations of each compound (10^{-12} – 10^{-3} M) and a fixed amount of radioligand (100 000 counts per minute).

^bSix independent experiments were run in quadruplicate.

Data are expressed as means ± SD (with ^c95% confidence limits).

reference compound BIO1211 and the hybrid α/β -peptides DS-70 and DS-23 blocked Jurkat E6.1 cell adhesion in the nanomolar range (Table 1).

DS-70 was more effective than DS-23 as an antagonist of $\alpha_4\beta_1$ integrin and we therefore focused our research efforts on this compound. First, we assessed whether DS-70 inhibited the adhesion of the human mast cell line HMC 1.1 and of the human eosinophilic cell line EoL-1, both of which mainly express $\alpha_4\beta_1$ integrin, to VCAM-1 or FN. This compound showed IC₅₀ values similar to the values observed in Jurkat E6.1 cells (Table 2).

The expression of α_4 integrin on the surface of Jurkat E6.1, EoL-1 and HMC 1.1 cell clones employed in this study was confirmed using a FITC-labelled anti α_4 antibody by flow cytometry. As reported in Figure S3, the three cell lines express consistent levels of this integrin on their surface. All the other cell lines employed for cell adhesion assays, as shown in Figure S3, do not express α_4 integrin.

Table 2

Effect of DS-70^a on different integrin-mediated human cell adhesion systems

Cell/integrin expressed	Adhesion molecule	IC ₅₀ (nM) ^b
HMC-1/ $\alpha_4\beta_1$	VCAM-1	8.4 ± 1.9 (0.1–32.4) ^c
EoL-1/ $\alpha_4\beta_1$	VCAM-1	9.7 ± 3.2 (1.2–38.6)
RPMI8860/ $\alpha_4\beta_7$	MAdCAM-1	70 ± 6.5 (6.9–260.8)
Jurkat/ $\alpha_L\beta_2$	ICAM-1	>5000
HL60/ $\alpha_M\beta_2$	Fibrinogen	>5000
K562/ $\alpha_5\beta_1$	FN	>5000
SK-MEL-24/ $\alpha_V\beta_3$	FN	>5000
MCF7/ $\alpha_V\beta_5$	Fibrinogen	>5000
HT-29/ $\alpha_V\beta_6$	FN	>5000
HEL/ $\alpha_{IIb}\beta_3$	Fibrinogen	>5000
D283/ $\alpha_9\beta_1$	FN	>5000

^aIn a cell-based assay, the adhesion of a cell line preferentially expressing a specific integrin heterodimer to an immobilized adhesion molecule was measured.

^bSix independent experiments were run in quadruplicate.

Data are expressed as means ± SD (with ^c95% confidence limits).

RPMI 8866 cells predominantly express the leukocyte integrin $\alpha_4\beta_7$, and the adhesion molecule MAdCAM-1 predominantly measures $\alpha_4\beta_7$ -mediated cell adhesion (Erle *et al.*, 1994). DS-70 was approximately eightfold less potent in blocking cell adhesion mediated by $\alpha_4\beta_7$ integrin binding to MAdCAM-1 in RPMI 8866 cells (Table 2) compared to VCAM-1 and FN-mediated cell adhesion in EoL-1 or HMC 1.1 cells. Furthermore, DS-70 did not inhibit cell adhesion mediated by the leukocyte integrins $\alpha_L\beta_2$ and $\alpha_M\beta_2$ or by the Arg-Gly-Asp-binding integrins $\alpha_5\beta_1$, $\alpha_V\beta_3$, $\alpha_V\beta_5$, $\alpha_V\beta_6$ and $\alpha_{IIb}\beta_3$ (Table 2). Taken together, these results confirm that DS-70 may behave as a competitive antagonist of cell adhesion molecules that preferentially bind to α_4 integrin.

In vitro enzymic stability of DS-70

The *in vitro* stability of DS-70 in mouse serum at 37°C was compared with BIO1211. As shown in Figure S4, BIO1211 had an approximate half-life of 0.27 ± 0.07 h (mean ± SD; $n = 5$). DS-70 was more stable, and after 8 h, 21 ± 2% of its content in serum had degraded. These data support the hypothesis that the presence of the β -amino acid scaffold markedly increased the enzymic stability of this peptidomimetic.

Effects of DS-70 on VCAM-1-mediated ERK 1/2 phosphorylation

Intracellular signalling generated by the interaction of components of the extracellular matrix with integrin $\alpha_4\beta_1$ involves second messengers such as ERK1/2 that contribute to α_4 integrin-mediated cell functions (Abdala-Valencia *et al.*, 2011). The addition of DS-70 alone to Jurkat E6.1 cells did not cause any significant increase in ERK 1/2 phosphorylation compared to vehicle-treated cells (data not shown). A significant increase in ERK 1/2 phosphorylation was detected 60 min after Jurkat E6.1 cells were exposed to VCAM-1-coated plates ($2 \mu\text{g}\cdot\text{mL}^{-1}$). Pre-incubation with DS-70 (10^{-10} – 10^{-4} M) for 60 min, produced a concentration-dependent decrease in VCAM-1-mediated ERK1/2 phosphorylation (Figure 2A,B). DS-70 was also effective in reducing, in a concentration-related manner, ERK 1/2 phosphorylation induced by VCAM-1 in HMC 1.1 and EoL-1 cells (Figure S5).

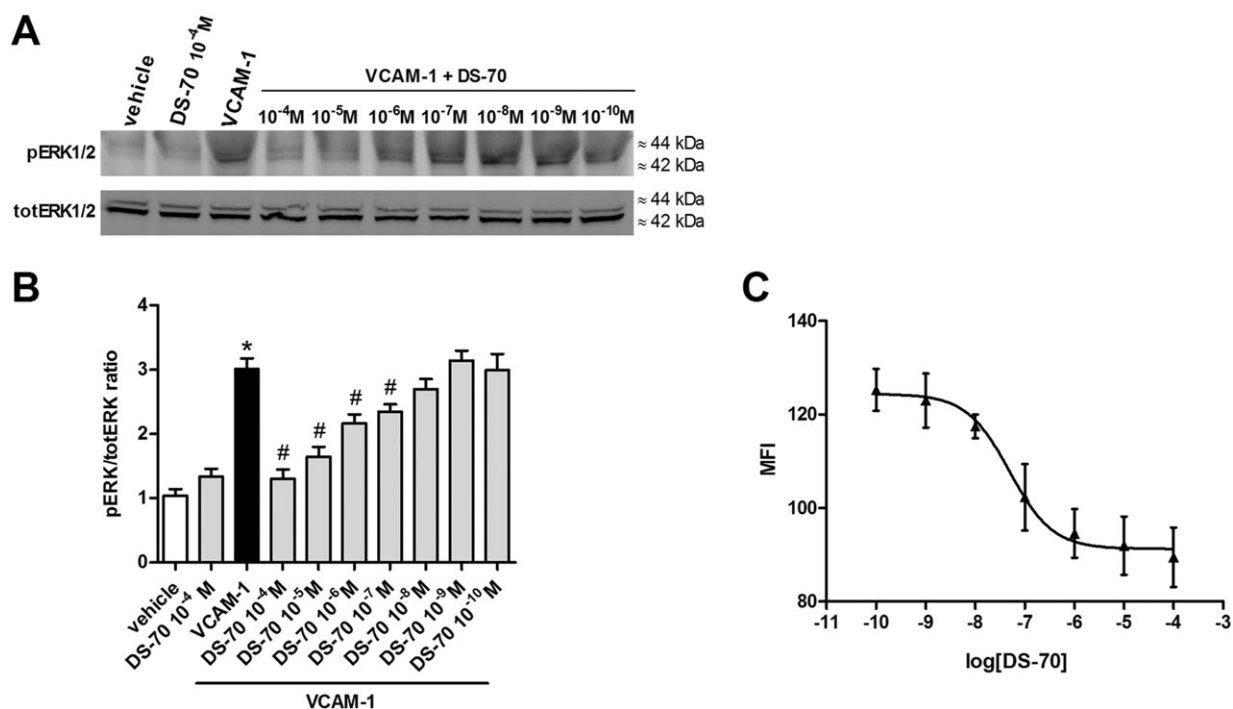


Figure 2

DS-70 reduces, in a concentration-related manner, VCAM-1-induced ERK 1/2 phosphorylation (pERK 1/2) in Jurkat E6.1 cells and VCAM-1 binding to Jurkat E6.1 cells exposed to PE-conjugated HUTS-21 mAb. (A) Jurkat E6.1 cell extracts were assayed for pERK 1/2 by Western blotting; a representative assay is shown. Control cells plated on VCAM-1 had a much stronger signal for pERK 1/2 than vehicle-treated cells. DS-70 reduces VCAM-1-induced pERK1/2, whereas, at a higher concentration (10^{-4} M), it was not able to modify pERK1/2 in the absence of this adhesion molecule. (B) The results of semiquantitative densitometry analysis of the bands from five independent experiments are shown (mean \pm SD); the amount of pERK 1/2 is normalized to that of total ERK 1/2. * $P < 0.05$, significantly different from vehicle; # $P < 0.05$, significantly different from VCAM-1. (C) Mean fluorescence intensity (MFI) due to the anti- β_1 integrin mAb PE conjugated HUTS-21 plotted against different concentrations of DS-70 added to Jurkat E6.1 cells in the presence of VCAM-1 ($5 \mu\text{g}\cdot\text{mL}^{-1}$) was measured. Each point represents the mean \pm SD of five independent experiments carried out in triplicate. VCAM-1 administered alone was able to promote epitope exposure and a significant increase of MFI over vehicle-treated cells exposed to PE conjugated HUTS-21 alone (MFI values were 130 ± 3 vs. 80 ± 4 ; $n = 5$, $P < 0.05$, significantly different from VCAM-1 alone. Non-specific binding of an isotype control PE conjugated mAb added to Jurkat E6.1 cells produced an MFI of 38 ± 4 ($n = 5$) that was subtracted from all samples.

DS-70 binding to $\alpha_4\beta_1$ integrin modulates HUTS-21 epitope exposure in Jurkat E6.1 cells

Integrins exist in three major conformations: an inactive or bent conformation, an intermediate-activity conformation and a high-activity open conformation (Margadant *et al.*, 2011). Conformational changes in integrin subunits may be monitored using conformation-specific antibodies that recognize a specific epitope that is exposed only in a defined structural conformation (Luque *et al.*, 1996). We used the PE-conjugated HUTS-21 mAb to determine whether the binding of DS-70 to $\alpha_4\beta_1$ integrin alters its conformation. This mAb recognizes a ligand-induced binding site epitope that is masked in the inactive integrin but is exposed upon agonist binding or partial integrin activation. The epitope recognized by HUTS-21 has been mapped to the hybrid domain of β_1 integrin (Luque *et al.*, 1996). This mAb was added to Jurkat E6.1 cells in the presence of VCAM-1 ($2 \mu\text{g}\cdot\text{mL}^{-1}$), and fluorescence was assayed using flow cytometry. As expected, HUTS-21 binds to β_1 integrin and exhibits increased Jurkat cell-associated fluorescence compared to the cells exposed to an isotype control mAb. The binding of $\alpha_4\beta_1$ integrin to its endogenous ligand VCAM-1 induces a conformational

rearrangement in the β_1 subunit that exposes the HUTS-21 epitope and increases antibody binding. As shown in Figure 2C, DS-70 (10^{-10} – 10^{-4} M) concentration-dependently reduced the exposure of the HUTS-21 epitope as it decreased mAb binding in the presence of VCAM-1 with an IC_{50} of 4.33×10^{-8} M. DS-70 alone (10^{-10} – 10^{-4} M) did not result in any significant exposure of the mAb epitope registered as an increase of fluorescence (data not shown). Thus, DS-70 seems to act as an $\alpha_4\beta_1$ integrin antagonist, as it favours the inactive and/or intermediate-activity conformations of this integrin.

DS-70 inhibits VCAM-1-mediated mast cell and eosinophil degranulation

Integrin α_4 plays a crucial role in allergic reactions because it is expressed on mast cells (Yasuda *et al.*, 1995; Hallgren and Gurish, 2011) and eosinophils (Barthel *et al.*, 2008). Integrin adhesion molecules are involved in the trafficking of inflammatory cells from the circulation into inflamed tissues (Kourtzelis *et al.*, 2017) and contribute to acute mast cell degranulation following allergen exposure (Hojo *et al.*, 1998). Consistent with this latter observation, VCAM-1 ($2 \mu\text{g}\cdot\text{mL}^{-1}$) caused significant degranulation of the human

mast cell line HMC 1.1, as assayed by measuring the release of β -hexosaminidase into the cell supernatant. This effect was prevented by exposing the cells to a mAb that binds to the $\alpha_4\beta_1$ integrin expressed on the cell surface.

Pretreatment with DS-70 (10^{-10} – 10^{-4} M) 60 min prior to VCAM-1 administration caused a concentration-dependent inhibition of VCAM-1-induced mast cell degranulation (Figure 3A).

VCAM-1 may interact with several cytokines to promote eosinophil recruitment during the initiation phase of inflammation, and the functional activation of eosinophils is characterized by degranulation (Nagata *et al.*, 1998). IL-5 plays a fundamental role in eosinophil differentiation in the bone marrow, as well as recruitment and activation at sites of allergic inflammation (Broughton *et al.*, 2015). Based on this premise, we found that VCAM-1 or IL-5 promote a significant EoL-1 degranulation by measuring the release of eosinophil peroxidase in cell culture medium. **IL-5**-induced release of eosinophil peroxidase was significantly increased following a 4 h incubation in VCAM-1-coated wells; this effect was blocked by a mAb that binds to α_4 integrin. DS-70 (10^{-10} – 10^{-4} M) prevents the IL-5-induced release of eosinophil peroxidase from cells maintained in VCAM-1-coated wells in a concentration-related manner whereas, when added to control cells, DS-70 was not effective (Figure 3B).

DS-70 does not promote cell apoptosis and necrosis

We analysed the capacity of DS-70 to induce apoptosis and necrosis in the three cell lines used in this study: Jurkat

E6.1, HMC 1.1 and EoL-1. Cells were treated with DS-70 (10^{-4} M) for 6 h, and cell apoptosis and/or necrosis were assessed by flow cytometry; we measured annexin V-PE fluorescence using 7-AAD-induced apoptotic cells as a positive control. As shown in Figure S6, DS-70 did not cause any significant apoptotic cell death in the three cell lines investigated. Compared with the control, the number of live cells did not decrease, and the percentages of early apoptotic cells, late apoptotic/secondary necrotic or damaged cells did not change in the presence of DS-70.

DS-70 eye drops reduce allergic reactions in guinea pigs and conjunctival α_4 integrin

Guinea pigs were actively immunized via i.p. administration of ovalbumin and challenged with ovalbumin instilled into the conjunctival sac 21 days later. One hour after challenge, during the early phase reaction, clinical observations revealed typical early phase symptoms of allergic conjunctivitis, such as tearing and discharge, conjunctival redness and chemosis. The mean clinical score reached the maximum 2 h after allergen challenge and thereafter showed a progressive decrease. At 24 h after challenge, the conjunctiva did not present any relevant clinical symptom (Baiula *et al.*, 2014).

The administration of DS-70 eye drops (0.01, 0.05 and 0.1%, w/v) in the conjunctival sac of both eyes (30 μ L per eye) of ovalbumin-sensitized guinea pigs 30 and 10 min before topical ovalbumin challenge reduced inflammatory signs observed in the early and late phases of conjunctival allergy

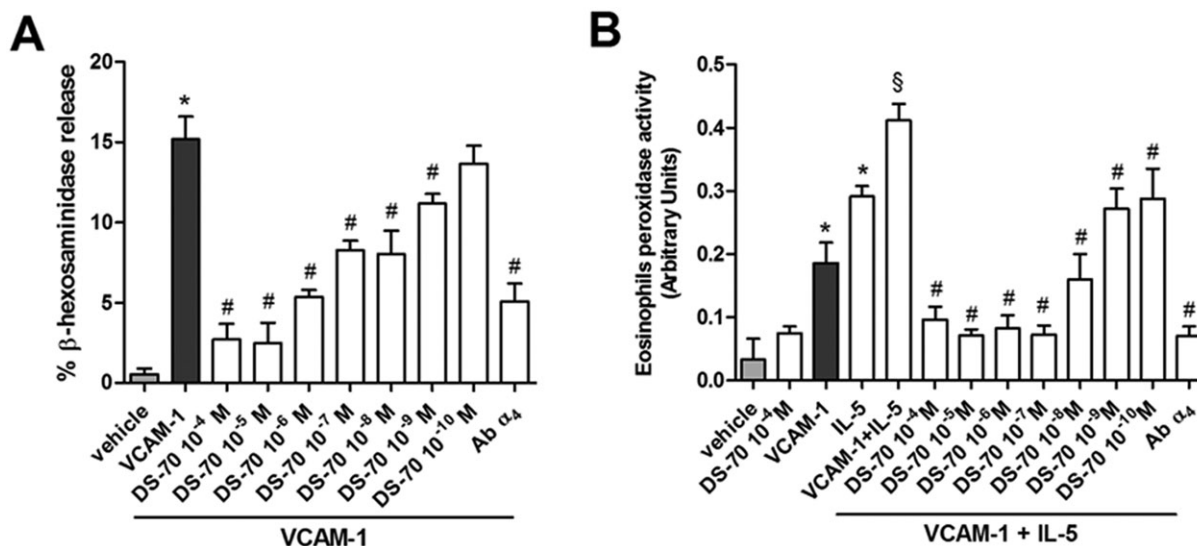


Figure 3

DS-70 antagonizes HMC1.1 cells degranulation and eosinophil peroxidase release from the eosinophilic EoL-1 cells. (A) In HMC1.1 cells seeded on VCAM-1 ($2 \mu\text{g}\cdot\text{mL}^{-1}$)-coated plates, a pronounced increase of β -hexosaminidase release is observed. DS-70 (10^{-10} – 10^{-4} M) concentration-dependently decreased β -hexosaminidase release. VCAM-1-induced β -hexosaminidase release is significantly prevented in cells treated with a monoclonal antibody anti- α_4 . Degranulation is expressed as percentage of β -hexosaminidase released over total content measured in cells lysed with Triton X-100. (B) VCAM-1 ($5 \mu\text{g}\cdot\text{mL}^{-1}$) exposure promotes a significant increase of eosinophil peroxidase release from EoL-1 cells and elevates IL-5 ($50 \text{ ng}\cdot\text{mL}^{-1}$)-induced release of this enzyme. DS-70 (10^{-4} – 10^{-10} M) added to the cells prior to exposure to VCAM-1 and IL-5 significantly reduces eosinophil peroxidase release. β -Hexosaminidase release caused by VCAM-1 + IL-5 is significantly prevented by pre-treatment with a monoclonal antibody anti- α_4 . Data are expressed as the mean \pm SD of five experiments carried out in triplicate. * $P < 0.05$, significantly different from vehicle; # $P < 0.05$, significantly different from VCAM-1 (panel A) or VCAM-1 + IL-5 (panel B); [§] $P < 0.05$, significantly different from IL-5.

in a dose-dependent manner. The 0.1% dose was the most effective. The topical administration of DS-70 eye drops (0.1%; administered twice 20 min apart) in control guinea pigs sensitized with saline did not cause any significant sign of discomfort or any conjunctival inflammatory symptoms (Figure 4).

A selective and sensitive LM-MS/MS method was developed for the analysis of DS-70 and the internal standard levocabastine hydrochloride in the guinea pig conjunctiva. Both the analyte and the internal standard had similar molecular weight and ClogP values. Adopting this procedure, DS-70 administered to the conjunctival fornix (30 μ L of

0.1 g·100 mL⁻¹) twice, 30 min apart, was detected in the conjunctiva 1 h after the first treatment (7780 \pm 1000 ng·g⁻¹ wet tissue). Interestingly, conjunctival DS-70 was also detected at lower levels, 6 h after the first treatment (3450 \pm 800 ng·g⁻¹ wet tissue).

The effects of DS-70 on allergic ocular conjunctivitis were compared to those induced by a reference drug dexamethasone (Figure S7). Dexamethasone eye drops (0.1%, w/v) administered to a separate group of guinea pigs sensitized and challenged with ovalbumin as described above produced a reduction of allergic conjunctivitis, superimposable on the effect elicited by DS-70 (0.1%) (Figure S7).

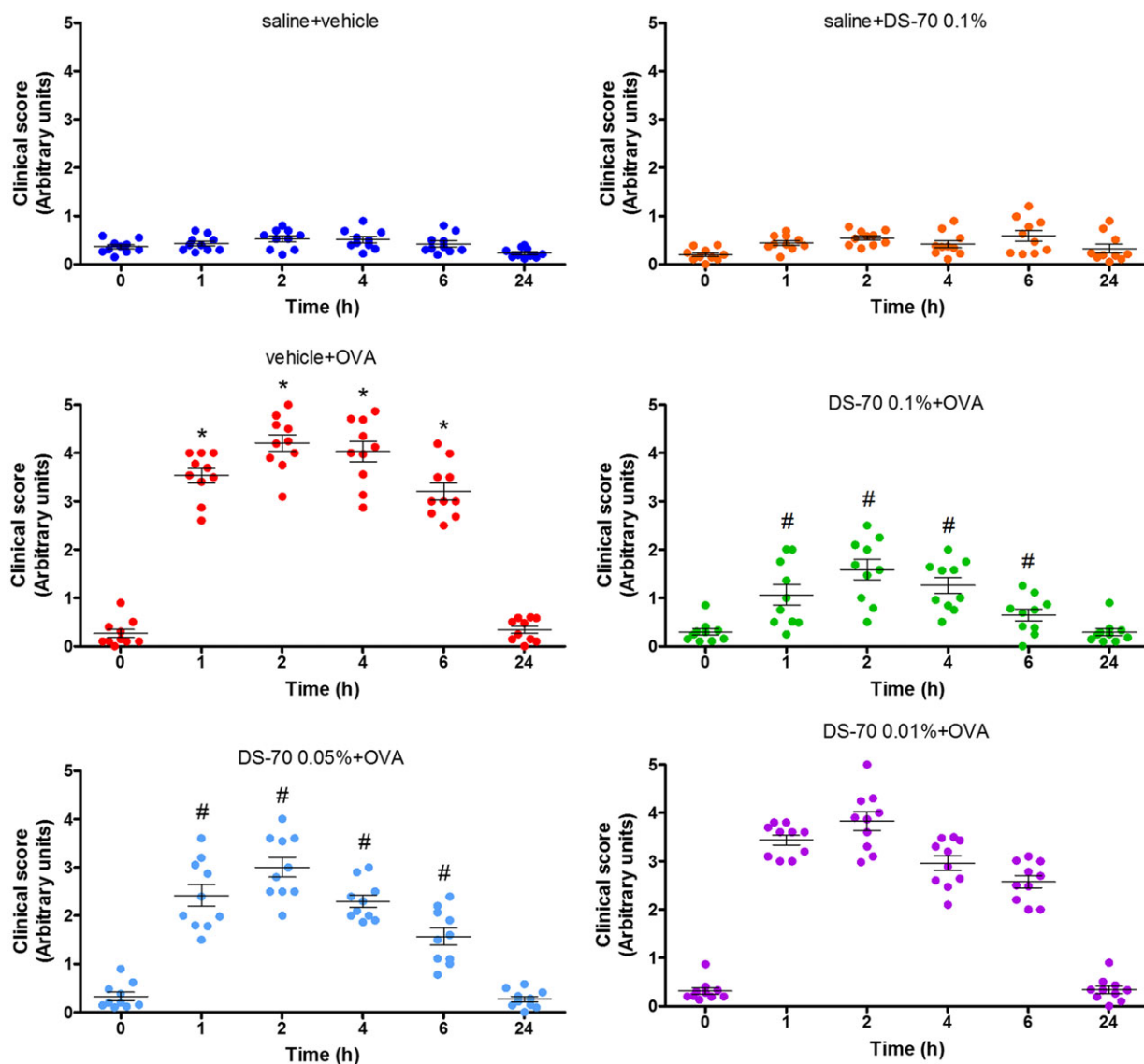


Figure 4

Effects of DS-70 on conjunctival symptoms induced by ovalbumin (OVA) in guinea pigs. Guinea pigs sensitized and challenged with ovalbumin and treated with the vehicle used to dissolve DS-70 (vehicle + OVA) responded with an increase in clinical score index. Administration of DS-70 significantly counteracts, in a dose-related manner, pathological signs and improves eye appearance. Data are presented as scatter plot and refer to the mean \pm SD (five animals per group were included, and both eyes were evaluated; $n = 10$). * $P < 0.05$, significantly different from saline + vehicle; # $P < 0.05$, significantly different from vehicle + OVA.

These data are in agreement with our previous paper (Baiula *et al.*, 2011).

Guinea pigs were killed 24 h later, and tissues were analysed histologically. Numerous mast cells infiltrating the lamina propria and stroma of the conjunctiva were observed, and most had degranulated in guinea pigs sensitized and challenged with ovalbumin. It was possible to recognize both metachromatic and degranulated mast cells with May–Grünwald–Giemsa staining (Figure S8A). In contrast to vehicle-treated guinea pigs, DS-70 caused a dose-dependent reduction in the number of infiltrating degranulated mast cells, and the majority were granulated mast cells (Figures 5A and S8A).

Similarly, eosinophil infiltration and eosinophil peroxidase activity, which are used as an index of the conjunctival infiltration of eosinophils (Qasem *et al.*, 2008), were increased in specimens of tarsal conjunctiva obtained from guinea pigs killed 24 h after antigen sensitization and challenge, whereas a notable, dose-dependent reduction in both parameters was observed in DS-70-treated guinea pigs (Figure 5B,C).

Exposure of ovalbumin-sensitized guinea pigs to the topical challenge of ovalbumin instilled into the conjunctival sac induced a significant increase in α_4 integrin levels in sections of tarsal conjunctiva after 24 h, as measured by immunohistochemistry. This increase may be a consequence of the elevated infiltration of leukocytes, such as eosinophils expressing this integrin in the conjunctiva, including mast cells. Interestingly, DS-70 significantly reduced α_4 integrin expression in conjunctival specimens obtained from treated guinea pigs in a dose-dependent manner (Figure 6).

Immunofluorescence analysis carried out on sections obtained from tarsal conjunctiva specimens of guinea pigs sensitized and challenged with ovalbumin showed a double

staining for tryptase, as marker of mast cells (Hojo *et al.*, 1998) and α_4 integrin. Moreover, the double staining of MBP, a marker of eosinophils (Nagata *et al.*, 1998), and α_4 integrin showed the presence of both proteins in specimens of tarsal conjunctiva (Figure S9). Numerous cells positive for double staining were observed, confirming that α_4 integrin is expressed on both mast cells and eosinophils localized in conjunctival specimens (Figure S9).

DS-70 eye drops reduce conjunctival levels of chemokine and cytokine mRNAs and protein content of CCL5 and CCL11 in ovalbumin-treated guinea pigs

Ovalbumin challenge in actively immunized guinea pigs induced a significant elevation of the levels of mRNAs for IL-8, IL-1 β , CCL5 and CCL11, and of protein levels of CCL5 and CCL11, in tarsal conjunctival specimens after 24 h. Pretreatment with DS-70 prior to ovalbumin challenge effectively and dose-dependently reduced the conjunctival levels of the cytokine and chemokine mRNAs (Figure 7) as well as CCL5 and CCL11 protein levels (Figure 8).

Discussion

In our continuing investigations of small molecules possessing the pharmacological profile of integrin antagonists, we designed and synthesized two novel peptidomimetics. DS-70 possesses a β -amino acid that contributes to increased serum stability compared to the reference $\alpha_4\beta_1$ integrin antagonist BIO1211 (Lin *et al.*, 1999). Furthermore, this component contributed to the stable conformation of the overall structure.

DS-70 prevents the adhesion of Jurkat E6.1 cells, an immortalized human T lymphocyte line, EoL-1 cells, a human

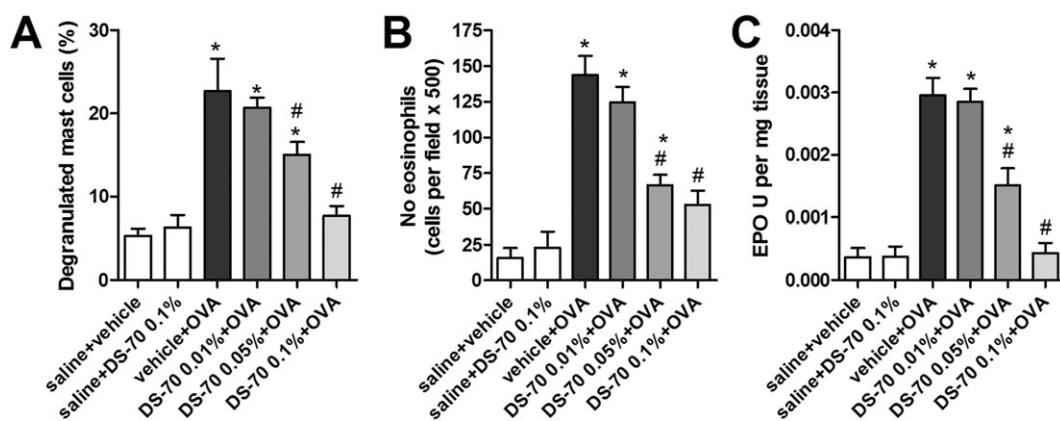


Figure 5

DS-70 prevents, in a dose-dependent manner, conjunctival infiltration and degranulation of mast cells and eosinophils. (A) The number of degranulated mast cells was evaluated in photographs taken of 10 random fields of 10 different conjunctival sections (see photomicrographs of tarsal conjunctiva stained with May–Grünwald–Giemsa shown in Figure S8A) and reported as percentage of degranulated mast cells (calculated with the following formula: $DMC/MC \times 100$). (B) Effects of DS-70 eye drops on conjunctival eosinophil infiltration 24 h after topical challenge with ovalbumin. Substantial eosinophil infiltration was observed in guinea pigs sensitized and topically challenged with ovalbumin. In guinea pigs sensitized with ovalbumin, treated with DS-70 eye drops and challenged with ovalbumin, there was a lower, dose-related, eosinophil infiltration than in conjunctiva of guinea pigs treated with ovalbumin alone. The number of eosinophils was determined in photographs taken of 10 random fields of 10 different sections (Luna's staining; see Figure S8B). (C) Effects of DS-70 eye drops on conjunctival eosinophil peroxidase levels 24 h after topical challenge with ovalbumin. Data refer to the mean \pm SD (five animals per group were included, and both eyes were evaluated; $n = 10$). * $P < 0.05$, significantly different from saline + vehicle; # $P < 0.05$, significantly different from vehicle + OVA.

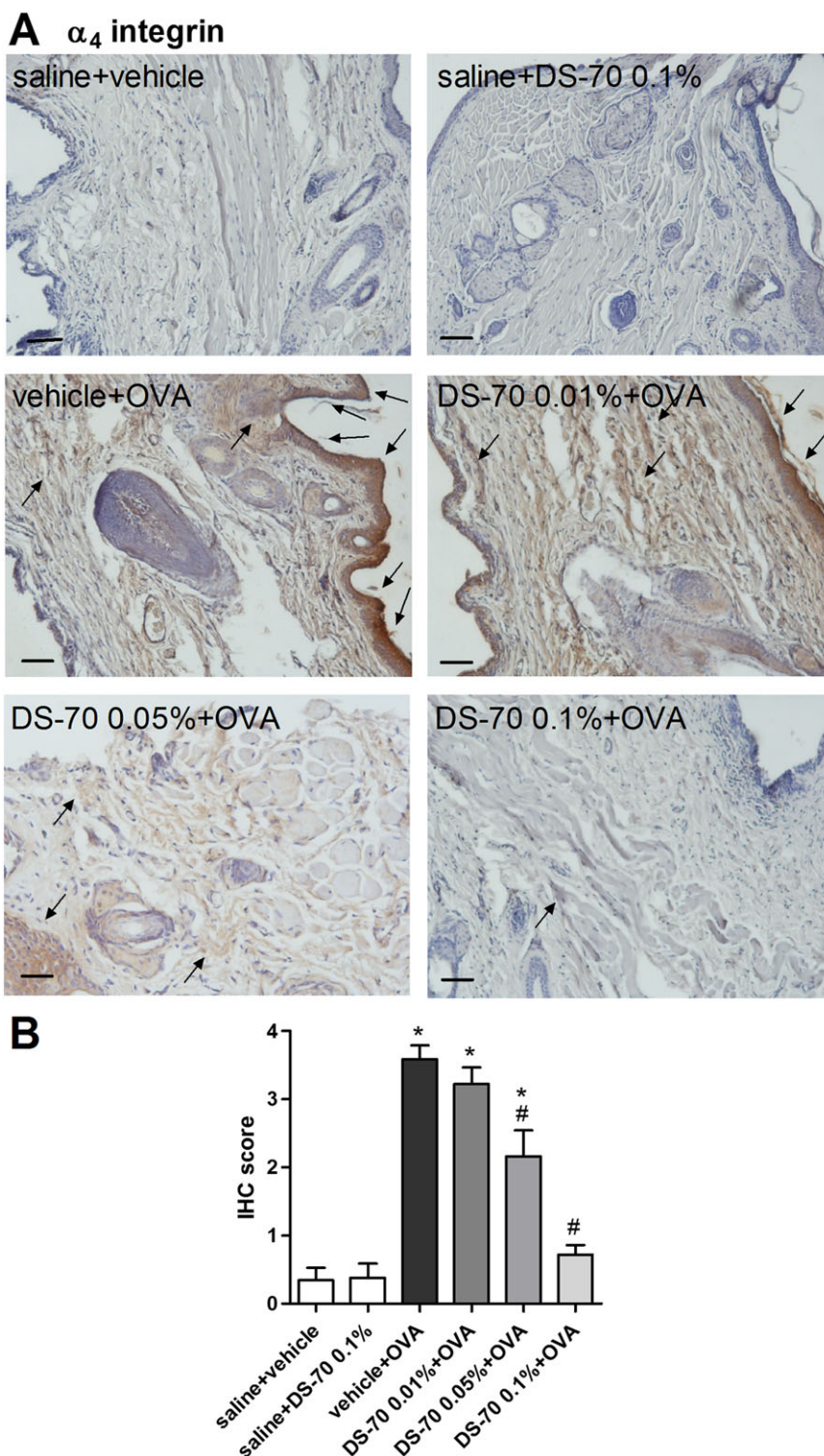


Figure 6

Topical treatment with DS-70 in guinea pigs sensitized and challenged with ovalbumin reduces conjunctival levels of α_4 integrin. (A) Photomicrographs of the conjunctiva 24 h after topical challenge with ovalbumin and pretreatment with DS-70 (0.01, 0.05 and 0.1%). Black arrows in panel A indicate hot spots of expression. (B) IHC score was assigned as reported in the Methods. Guinea pigs sensitized with saline and treated with the vehicle used to dissolve DS-70 (saline + vehicle) showed basal levels of expression, as animals sensitized with saline and treated with DS-70 alone (saline + DS-70 0.1%). In guinea pigs sensitized and challenged with ovalbumin and treated with the vehicle used to dissolve DS-70 (vehicle + OVA), IHC score is markedly increased, and DS-70 at the concentration 0.1% maximized the reduction that can be seen already observed at 0.05%. Data are presented as the mean \pm SD (five animals per group were included, and both eyes were evaluated; $n = 10$). Black bars = 50 μ m. * $P < 0.05$, significantly different from saline + vehicle; # $P < 0.05$, significantly different from vehicle + OVA.

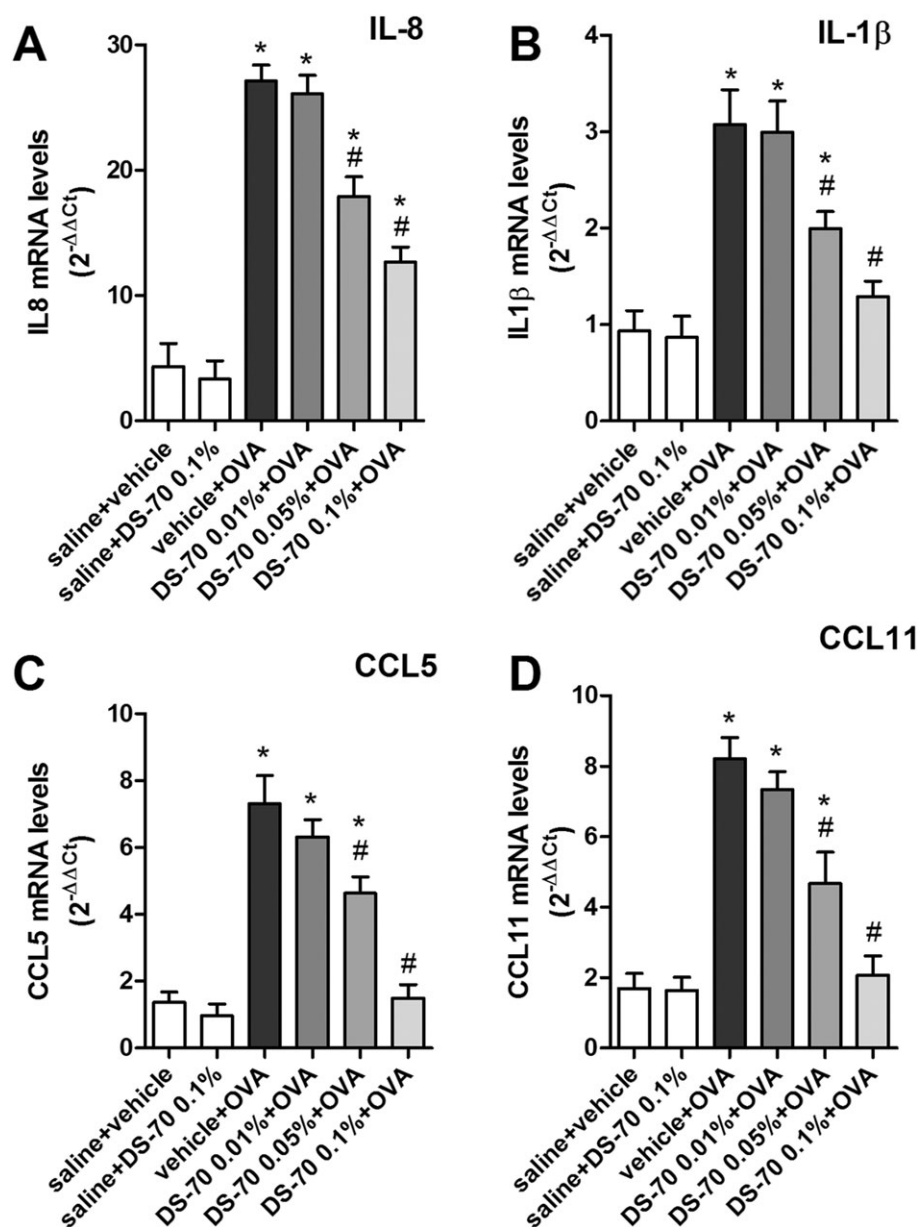


Figure 7

DS-70 eye drops (0.1% suspension) induced a significant down-regulation of IL-8, IL-1 β , CCL5 and CCL11 transcripts in conjunctiva. Relative fold changes in mRNA levels were calculated using the $\Delta\Delta C_t$ method as described in the Methods. Ovalbumin challenged animals (vehicle + OVA) behave as positive control; DS-70 0.05% and DS-70 0.1% reduce this increase. Values are the mean \pm SD (five animals per group were included, and both eyes were evaluated; $n = 10$). * $P < 0.05$, significantly different from saline + vehicle; # $P < 0.05$, significantly different from vehicle + OVA.

eosinophilic leukaemia cell line, and HMC 1.1 cells, a human mast cell line, all of which express integrin $\alpha_4\beta_1$, to VCAM-1 and FN. Although DS-70 is eightfold less potent in preventing the adhesion of RPMI 8866 cells that express $\alpha_4\beta_7$ (Erle *et al.*, 1994) to MAdCAM-1 than cells that express $\alpha_4\beta_1$ integrin, DS-70 still prevents adhesion in the nanomolar range. Thus, this novel compound may be considered a dual antagonist of $\alpha_4\beta_1/\alpha_4\beta_7$ integrins. We further characterized DS-70 as an effective antagonist of α_4 integrin by showing that it antagonized VCAM-1-mediated phosphorylation of ERK 1/2 in Jurkat E6.1 cells and VCAM-1-mediated degranulation of HMC 1.1 mast cells and EoL-1 cells.

Consistent with other studies (Karanam *et al.*, 2007), the reference $\alpha_4\beta_1$ integrin antagonist BIO1211 is metabolically unstable when added to mouse serum *in vitro* ($t_{1/2} = 2.1$ h), whereas only 21% of DS-70 was degraded under the same experimental conditions. These data further confirm the potential for DS-70 to be developed as drug for administration *in vivo*. Following administration of DS-70 in the guinea pig conjunctival fornix, it was detected in the conjunctiva. Higher levels were measured 1 h later, but it was still present 6 h after treatment. These data provide more evidence for the antiallergic effects that this agent promotes at conjunctival level.

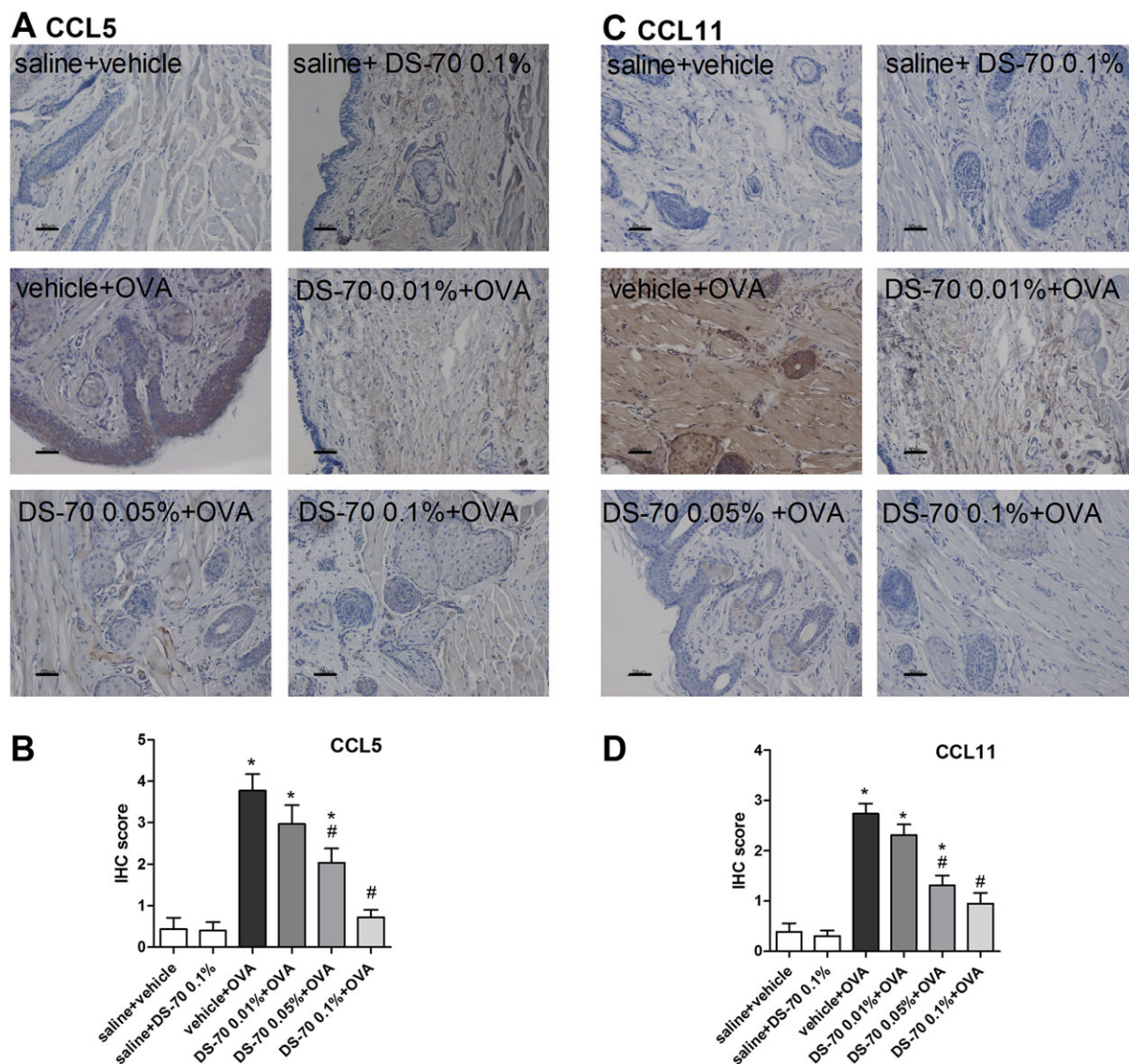


Figure 8

DS-70 reduces CCL5 and CCL11 conjunctival expression. Conjunctival sections were examined by IHC for the expression of chemokines and the IHC scores calculated. (A–C) Representative photographs stained with specific primary antibodies are shown. (B–D) IHC scores assigned. Tissue sections from guinea pigs treated with saline (saline + vehicle) and DS-70 alone (saline + DS-70 0.1%) were used as a negative control. Scale bar, 50 μ m. Data are presented as mean \pm SD (five animals per group were included, and both eyes were evaluated; $n = 10$). * $P < 0.05$, significantly different from saline + vehicle; # $P < 0.05$, significantly different from vehicle + OVA.

Using the mAb PE conjugated HUTS-21 that recognizes a ligand-induced binding site epitope of β_1 integrin expressed with the α_4 subunit (Luque *et al.*, 1996), DS-70 concentration-dependently reduced the exposure of HUTS-21 epitope, as measured by mAb binding in the presence of the endogenous $\alpha_4\beta_1$ agonist VCAM-1. Finally, in a model of allergic conjunctivitis, DS-70 eye drops dose-dependently antagonized the clinical symptoms of conjunctival allergy and the conjunctival expression of α_4 integrin by reducing infiltration of leukocytes, such as eosinophils expressing this integrin in the conjunctiva, including mast cells.

The $\alpha_4\beta_1$ integrin/VCAM-1 pathway seems to be crucial for the firm adhesion and transmigration of mast cells

(Parmley *et al.*, 2007) and eosinophils (Nagata *et al.*, 1998) into the conjunctiva through vascular endothelial cells. The inhibition of conjunctival eosinophil infiltration by an integrin mAb has been reported in a guinea pig model of allergic conjunctivitis (Ebihara *et al.*, 1999). Furthermore, treatment with anti- α_4 integrin and anti-VCAM-1 antibodies significantly suppressed the conjunctival eosinophil infiltration induced in mice following active immunization with ragweed or adoptive transfer of ragweed-primed splenocytes (Fukushima *et al.*, 2006). As shown by Higashimoto *et al.* (1999), the adhesion of eosinophils to FN is mediated by $\alpha_4\beta_1$ integrin, potentially contributing to the increased cell adhesion to the extracellular matrix and conjunctival eosinophil accumulation.

These *in vitro* data may help to explain the reduction in the expression of α_4 integrin observed in the conjunctiva of ovalbumin-sensitized guinea pigs treated with DS-70. In fact, this effect might be a consequence of the DS-70-mediated reduction in the recruitment and migration of mast cells and eosinophils to the site of allergic inflammation, rather than of the down-regulation of $\alpha_4\beta_1$ induced by DS-70. This hypothesis is further supported by the findings that integrins increase their affinity or avidity for endothelial-expressed adhesion molecules upon exposure to chemokines and undergo conformational changes upon ligand binding in addition to changes in their expression on the leukocyte surface (Hyduk and Cybulsky, 2009).

We ascertained the positive effect of DS-70 eye drops on inflammatory changes induced by allergen-specific conjunctival challenge. This novel molecule, topically administered prior to ovalbumin challenge, effectively and dose-dependently reduced the conjunctival levels of the cytokines IL-1 β and IL-8 and of the chemokines CCL5 and CCL11 at both mRNA and protein levels. Histamine and eicosanoids are responsible for the typical early phase response (Katelaris, 2003). However, mast cells also contribute to the synthesis and release of cytokines, chemokines and growth factors, triggering a cascade of inflammatory events on the surface of epithelial and endothelial cells that leads to the late phase reaction, along with the recruitment of eosinophils and neutrophils (Abelson *et al.*, 2015). These latter cytokines participate in the production of chemokines, including CCL5 and CCL11, from conjunctival cells. The chemokine gradient regulates the trafficking of neutrophils, eosinophils and lymphocytes to the conjunctiva occurring during the late phase. CCL5 and CCL11 are included among major eosinophil chemoattractants. Furthermore, they are produced by eosinophils and are released during allergic responses. Mast cells express receptors for CCL5 and CCL11 and other chemokines that induce mast cell activation contributing to ongoing cellular infiltration and conjunctival hyperresponsiveness of the late phase (Komi *et al.*, 2018). Inflammatory cytokines may also enhance the expression of E-selectin, ICAM-1 and VCAM-1 on vascular endothelial cells and initiate the rolling and adhesion of immune cells (Bacon *et al.*, 1998).

By reducing mast cell degranulation, DS-70 eye drops may decrease the early phase response in ovalbumin-challenged guinea pigs and contribute to the conjunctival eosinophil infiltration in the late phase response. Consequently, conjunctival levels of cytokine and chemokine mRNAs are decreased (Pacharn and Vichyanond, 2013). These effects are further supported by α_4 integrin localized on conjunctival mast cells and eosinophils. Conjunctival epithelial cells do not express $\alpha_4\beta_1$ integrin (Fujihara *et al.*, 1997), and its expression in the conjunctiva may be derived from infiltrated inflammatory cells and promoted by different mechanisms.

According to serum stability studies and detection of topically applied DS-70 in the conjunctiva, it may be absorbed by conjunctival blood vessels and may persist at an adequate conjunctival concentration for up to 6–8 h, a sufficient period to interfere with mast cell activation and eosinophil migration to the ocular surface. We propose DS-70 as a novel α_4 integrin antagonist capable of relieving symptoms of allergic conjunctivitis in an appropriate animal model, and some of the targets of this drug include the conjunctival infiltration

of mast cells and eosinophils and the reduction of α_4 integrin expression.

Acknowledgements

This work was supported in part by grants from the University of Bologna FARB (FFBO 125290), RFO 2014 and RFO 2015; from MIUR (PRIN 2010); and from a research grant from Chiesi Foundation Onlus (Parma, Italy).

Author contributions

S.D.D. and M.B. conceived the study, designed the experiments, carried out the majority of the work and analysed the data. R.D.M., M.A. and L.G. designed, synthesized and analysed the chemical compounds. A.B. contributed to design the experiments, carried out part of the *in vitro* studies, performed *in vivo* experiments and contributed to analyse the data. L.G. and S.S. designed the study and wrote the manuscript. All the authors revised and approved the final version of the manuscript.

Conflict of interest

The authors declare no conflicts of interest.

Declaration of transparency and scientific rigour

This Declaration acknowledges that this paper adheres to the principles for transparent reporting and scientific rigour of preclinical research recommended by funding agencies, publishers and other organisations engaged with supporting research.

References

- Abdala-Valencia H, Berdnikovs S, Cook-Mills JM (2011). Mechanisms for vascular cell adhesion molecule-1 activation of ERK1/2 during leukocyte transendothelial migration. *PLoS One* 6: e26706.
- Abelson MB, Shetty S, Korchak M, Butrus SI, Smith LM (2015). Advances in pharmacotherapy for allergic conjunctivitis. *Expert Opin Pharmacother* 16: 1219–1231.
- Abu el-Asrar AM, Geboes K, al-Kharashi S, Tabbara KF, Missotten L, Desmet V (1997). Adhesion molecules in vernal keratoconjunctivitis. *Br J Ophthalmol* 81: 1099–1106.
- Ahmadzai M, Small M, Sehmi R, Gauvreau G, Janssen LJ (2015). Integrins are mechanosensors that modulate human eosinophil activation. *Front Immunol* 6: 525.
- Alexander SP, Fabbro D, Kelly E, Marrion N, Peters JA, Benson HE *et al.* (2015). The Concise Guide to PHARMACOLOGY 2015/16: Catalytic receptors. *Br J Pharmacol* 172: 5979–6023.

- Alexander SPH, Fabbro D, Kelly E, Marrion NV, Peters JA, Faccenda E *et al.* (2017). The Concise Guide to PHARMACOLOGY 2017/18: Enzymes. *Br J Pharmacol* 174: S272–S359.
- Awwad S, Mohamed Ahmed AHA, Sharma G, Heng JS, Khaw PT, Brocchini S *et al.* (2017). Principles of pharmacology in the eye. *Br J Pharmacol* 174: 4205–4223. <https://doi.org/10.1111/bph.14024>.
- Bacon AS, McGill JI, Anderson DF, Baddeley S, Lightman SL, Holgate ST (1998). Adhesion molecules and relationship to leukocyte levels in allergic eye disease. *Invest Ophthalmol Vis Sci* 39: 322–330.
- Baiula M, Bedini A, Baldi J, Cavet ME, Govoni P, Spampinato S (2014). Mapracorat, a selective glucocorticoid receptor agonist, causes apoptosis of eosinophils infiltrating the conjunctiva in late-phase experimental ocular allergy. *Drug Des Devel Ther* 8: 745–757.
- Baiula M, Bedini A, Carbonari G, Dattoli SD, Spampinato S (2012). Therapeutic targeting of eosinophil adhesion and accumulation in allergic conjunctivitis. *Front Pharmacol* 3: 203.
- Baiula M, Galletti P, Martelli G, Soldati R, Belvisi L, Civera M *et al.* (2016). New β -lactam derivatives modulate cell adhesion and signaling mediated by RGD-binding and leukocyte integrins. *J Med Chem* 59: 9721–9742.
- Baiula M, Spampinato S (2014). Phase II drugs under investigation for allergic conjunctivitis. *Expert Opin Investig Drugs* 23: 1671–1686.
- Baiula M, Spartà A, Bedini A, Carbonari G, Bucolo C, Ward KW *et al.* (2011). Eosinophil as a cellular target of the ocular anti-allergic action of mapracorat, a novel selective glucocorticoid receptor agonist. *Mol Vis* 17: 3208–3223.
- Barthel SR, Johansson MW, McNamee DM, Mosher DF (2008). Roles of integrin activation in eosinophil function and the eosinophilic inflammation of asthma. *J Leukoc Biol* 83: 1–12.
- Bedini A, Baiula M, Spampinato S (2008). Transcriptional activation of human mu-opioid receptor gene by insulin-like growth factor-I in neuronal cells is modulated by the transcription factor REST. *J Neurochem* 105: 2166–2178.
- Broughton SE, Nero TL, Dhagat U, Kan WL, Hercus TR, Tvorogov D *et al.* (2015). The β c receptor family – structural insights and their functional implications. *Cytokine* 74: 247–258.
- Choi SH, Bielory L (2008). Late-phase reaction in ocular allergy. *Curr Opin Allergy Clin Immunol* 8: 438–444.
- Contreras-Ruiz L, Mir FA, Turpie B, Krauss AH, Masli S (2016). Sjögren's syndrome associated dry eye in a mouse model is ameliorated by topical application of integrin α 4 antagonist GW559090. *Exp Eye Res* 143: 1–8.
- Cortijo J, Sanz MJ, Iranzo A, Montesinos JL, Nabah YN, Alfón J *et al.* (2006). A small molecule, orally active, α 4 β 1/ α 4 β 7 dual antagonist reduces leukocyte infiltration and airway hyper-responsiveness in an experimental model of allergic asthma in Brown Norway rats. *Br J Pharmacol* 147: 661–670.
- Curtis MJ, Alexander S, Cirino G, Docherty JR, George CH, Giembycz MA *et al.* (2018). Experimental design and analysis and their reporting II: updated and simplified guidance for authors and peer reviewers. *Brit J Pharmacol* 175: 987–993.
- Dattoli SD, De Marco R, Baiula M, Spampinato S, Greco A, Tolomelli A *et al.* (2014). Synthesis and assay of retro- α 4 β 1 integrin-targeting motifs. *Eur J Med Chem* 73: 225–232.
- De Marco R, Mazzotti G, Dattoli SD, Baiula M, Spampinato S, Greco A *et al.* (2015). 5-aminomethylloxazolidine-2,4-dione hybrid α/β -dipeptide scaffolds as inducers of constrained conformations: applications to the synthesis of integrin antagonists. *Biopolymers* 104: 636–649.
- De Marco R, Tolomelli A, Juaristi E, Gentilucci L (2016). Integrin ligands with α/β -hybrid peptide structure: design, bioactivity, and conformational aspects. *Med Res Rev* 36: 389–424.
- Ebihara N, Yokoyama T, Kimura T, Nakayasu K, Okumura K, Kanai A *et al.* (1999). Anti VLA-4 monoclonal antibody inhibits eosinophil infiltration in allergic conjunctivitis model of guinea pig. *Curr Eye Res* 19: 20–25.
- Ecoiffier T, El Annan J, Rashid S, Schaumberg D, Dana R (2008). Modulation of integrin α 4 β 1 (VLA-4) in dry eye disease. *Arch Ophthalmol* 126: 1695–1699.
- Erle DJ, Briskin MJ, Butcher EC, Garcia-Pardo A, Lazarovits AI, Tidswell M (1994). Expression and function of the MAdCAM-1 receptor, integrin α 4 β 7, on human leukocytes. *J Immunol* 153: 517–528.
- Fujihara T, Takeuchi T, Saito K, Tsubota K (1997). Flow cytometric analysis of surface antigens on human conjunctival epithelial cells. *Ophthalmic Res* 29: 103–109.
- Fukushima A, Yamaguchi T, Ishida W, Fukata K, Ueno H (2006). Role of VLA-4 in the development of allergic conjunctivitis in mice. *Mol Vis* 12: 310–317.
- Gentilucci L, Gallo F, Meloni F, Mastandrea M, Del Secco B, De Marco R (2016). Controlling cyclopeptide backbone conformation with β/α -hybrid peptide–heterocycle scaffolds. *Eur J Org Chem* 19: 3243–3251.
- George CH, Stanford SC, Alexander S, Cirino G, Docherty JR, Giembycz MA *et al.* (2017). Updating the guidelines for data transparency in the British Journal of Pharmacology – data sharing and the use of scatter plots instead of bar charts. *Br J Pharmacol* 174: 2801–2804.
- Groneberg DA, Bielory L, Fischer A, Bonini S, Wahn U (2003). Animal models of allergic and inflammatory conjunctivitis. *Allergy* 58: 1101–1113.
- Harding SD, Sharman JL, Faccenda E, Southan C, Pawson AJ, Ireland S *et al.* (2018). The IUPHAR/BPS guide to PHARMACOLOGY in 2018: updates and expansion to encompass the new guide to IMMUNOPHARMACOLOGY. *Nucl Acids Res* 46: D1091–D1106.
- Hallgren J, Gurish MF (2011). Mast cell progenitor trafficking and maturation. *Adv Exp Med Biol* 716: 14–28.
- Higashimoto I, Chihara J, Kawabata M, Nakajima S, Osame M (1999). Adhesion to fibronectin regulates expression of intercellular adhesion molecule-1 on eosinophilic cells. *Int Arch Allergy Immunol* 120 (Suppl. 1): 34–37.
- Hojo M, Maghni K, Issekutz TB, Martin JG (1998). Involvement of α -4 integrins in allergic airway responses and mast cell degranulation in vivo. *Am J Respir Crit Care Med* 158: 1127–1133.
- Hyduk SJ, Cybulsky MI (2009). Role of α 4 β 1 integrins in chemokine-induced monocyte arrest under conditions of shear stress. *Microcirculation* 16: 17–30.
- Irkec MT, Bozkurt B (2012). Molecular immunology of allergic conjunctivitis. *Curr Opin Allergy Clin Immunol* 12: 534–539.
- Iyer GR, Cason MM, Womble SW, Li G, Chastain JE (2015). Ocular pharmacokinetics comparison between 0.2% olopatadine and 0.77% olopatadine hydrochloride ophthalmic solutions administered to male New Zealand white rabbits. *J Ocul Pharmacol Ther* 31: 204–210.
- Jung EY, Ohshima Y, Shintaku N, Sumimoto S, Heike T, Katamura K *et al.* (1994). Effects of cyclic AMP on expression of LFA-1, Mac-1, and VLA-4 and eosinophilic differentiation of a human leukemia cell line, EoL-1. *Eur J Haematol* 53: 156–162.

- Karanam BV, Jayraj A, Rabe M, Wang Z, Keohane C, Strauss J *et al.* (2007). Effect of enalapril on the *in vitro* and *in vivo* peptidyl cleavage of a potent VLA-4 antagonist. *Xenobiotica* 37: 487–502.
- Katelaris CH (2003). Ocular allergy: implications for the clinical immunologist. *Ann Allergy Asthma Immunol* 90 (Suppl. 3): 23–27.
- Kenyon NJ, Liu R, O’Roark EM, Huang W, Peng L, Lam KS (2009). An $\alpha_4\beta_1$ integrin antagonist decreases airway inflammation in ovalbumin-exposed mice. *Eur J Pharmacol* 603: 138–146.
- Kilkenny C, Browne W, Cuthill IC, Emerson M, Altman DG, NC3Rs Reporting Guidelines Working Group (2010 Aug). Animal research: reporting *in vivo* experiments: the ARRIVE guidelines. *Br J Pharmacol* 160: 1577–1579.
- Komi EAD, Rambasek T, Bielory L (2018). Clinical implications of mast cell involvement in allergic conjunctivitis. *Allergy* 73: 528–539.
- Kourtzelis I, Mitroulis I, von Renesse J, Hajishengallis G, Chavakis T (2017). From leukocyte recruitment to resolution of inflammation: the cardinal role of integrins. *J Leukoc Biol* 102: 677–683.
- Kummer C, Ginsberg MH (2006). New approaches to blockade of α_4 -integrins, proven therapeutic targets in chronic inflammation. *Biochem Pharmacol* 72: 1460–1468.
- Lin K, Ateeq HS, Hsiung SH, Chong LT, Zimmerman CN, Castro A *et al.* (1999). Selective, tight-binding inhibitors of integrin $\alpha_4\beta_1$ that inhibit allergic airway responses. *J Med Chem* 42: 920–934.
- Luque A, Gómez M, Puzon W, Takada Y, Sánchez-Madrid F, Cabañas C (1996). Activated conformations of very late activation integrins detected by a group of antibodies (HUTS) specific for a novel regulatory region (355–425) of the common beta 1 chain. *J Biol Chem* 271: 11067–11075.
- McGrath JC, Lilley E (2015). Implementing guidelines on reporting research using animals (ARRIVE etc.): new requirements for publication in BJP. *Br J Pharmacol* 172: 3189–3193.
- Margadant C, Monsuur HN, Norman JC, Sonnenberg A (2011). Mechanisms of integrin activation and trafficking. *Curr Opin Cell Biol* 23: 607–614.
- Nagata M, Sedgwick JB, Kita H, Busse WW (1998). Granulocyte macrophage colony-stimulating factor augments ICAM-1 and VCAM-1 activation of eosinophil function. *Am J Respir Cell Mol Biol* 19: 158–166.
- Oh JW, Shin JC, Jang SJ, Lee HB (1999). Expression of ICAM-1 on conjunctival epithelium and ECP in tears and serum from children with allergic conjunctivitis. *Ann Allergy Asthma Immunol* 82: 579–585.
- Okada N, Fukagawa K, Takano Y, Dogru M, Tsubota K, Fujishima H *et al.* (2005). The implications of the upregulation of ICAM-1/VCAM-1 expression of corneal fibroblasts on the pathogenesis of allergic keratopathy. *Invest Ophthalmol Vis Sci* 46: 4512–4518.
- Pacham P, Vichyanond P (2013). Immunomodulators for conjunctivitis. *Curr Opin Allergy Clin Immunol* 13: 550–557.
- Parmley LA, Elkins ND, Fini MA, Liu YE, Repine JE, Wright RM (2007). $\alpha_4\beta_1$ and $\alpha_4\beta_2$ integrins mediate cytokine induced lung leukocyte-epithelial adhesion and injury. *Br J Pharmacol* 152: 915–929.
- Qasem AR, Bucolo C, Baiula M, Spartà A, Govoni P, Bedini A *et al.* (2008). Contribution of $\alpha_4\beta_1$ integrin to the antiallergic effect of levocabastine. *Biochem Pharmacol* 76: 751–762.
- Sperr WR, Agis H, Czerwenka K, Klepetko W, Kubista E, Boltz-Nitulescu G *et al.* (1992). Differential expression of cell surface integrins on human mast cells and human basophils. *Ann Hematol* 65: 10–16.
- Sundström M, Vliagoftis H, Karlberg P, Butterfield JH, Nilsson K *et al.* (2003). Functional and phenotypic studies of two variants of a human mast cell line with a distinct set of mutations in the *c-kit* proto-oncogene. *Immunology* 108: 89–97.
- Tolomelli A, Baiula M, Viola A, Ferrazzano L, Gentilucci L *et al.* (2015). Dehydro- β -proline containing $\alpha_4\beta_1$ integrin antagonists: stereochemical recognition in ligand-receptor interplay. *ACS Med Chem Lett* 6: 701–706.
- Walker RA (2006). Quantification of immunohistochemistry—issues concerning methods, utility and semiquantitative assessment I. *Histopathology* 49: 406–410.
- Yasuda M, Hasunuma Y, Adachi H, Sekine C, Sakanishi T, Hashimoto H *et al.* (1995). Expression and function of fibronectin binding integrins on rat mast cells. *Int Immunol* 7: 251–258.
- Wright N, Hidalgo A, Rodríguez-Frade JM, Soriano SF, Mellado M *et al.* (2002). The chemokine stromal cell-derived factor-1 α modulates $\alpha_4\beta_7$ integrin-mediated lymphocyte adhesion to mucosal addressin cell adhesion molecule-1 and fibronectin. *J Immunol* 168: 5268–5277.

Supporting Information

Additional supporting information may be found online in the Supporting Information section at the end of the article.

<https://doi.org/10.1111/bph.14458>

Figure S1 Relevant steps of the synthesis designed for DS-70 (A) and DS-23 (B) compounds, as described in the Methods.

Figure S2 [125 I]-FN binds to the complex between $\alpha_4\beta_1$ integrin and the antibody anti- α_4 integrin in the presence of scintillation beads coated with an anti-rabbit IgG antibody (the procedure is described in the Methods). (A) Representative autoradiogram of a western blot experiment, evaluating, separately, α_4 and β_1 integrin subunits in cell lysate fractions (1–4) of Jurkat E6.1 cells, expressing $\alpha_4\beta_1$ integrin. Fractions 1–4 were used in the SPA assays. (B) Saturation SPA binding of [125 I]-FN to $\alpha_4\beta_1$ integrin extracted and purified from Jurkat E6.1 cells and incubated with antibody anti- α_4 integrin, scintillation beads coated with the anti-rabbit IgG antibody and the radioligand. Non-specific binding was determined in the presence of increasing concentrations of [125 I]-FN (1–25 nM) and of 100 nM BIO1211. Saturation specific binding was determined by subtracting the non-specific binding from total binding counts. [125 I]-FN bound was expressed as counts per minute (cpm). Data are presented as mean \pm SEM of five experiments in triplicate.

Figure S3 Flow cytometry plots (number of cells count vs. green fluorescence) showing relative surface expression of integrin α_4 (filled peak) on all cell lines employed in *in vitro* experiments 4 compared with isotype control mAb (negative controls, empty peak). The fluorescence shifts reported for Jurkat E6.1, EoL-1 and HMC 1.1 cells confirmed that these cell lines strongly express α_4 integrin on their surface, while all other cell lines do not express α_4 integrin. A representative result of five independent experiments carried out in triplicate ($n = 5$) is shown.

Figure S4 Degradation of BIO1211 and DS-70 in mouse serum. Samples were removed from the incubation solution at 0, 0.15, 0.5, 1.0, 2.0, 4.0, 6.0 and 8.0 h and peptide stability was determined using an RP-HPLC ESI-MS analysis (described in the Methods). Values are presented as mean \pm SD ($n = 5$).

Figure S5 Effects of DS-70 on ERK 1/2 phosphorylation mediated by VCAM-1 in HMC1.1 (A, B) and EoL-1 cells (C, D). (A, C) Representative Western blots confirmed that VCAM-1 is able to induce ERK 1/2 phosphorylation in both cell lines and DS-70 maintains its inhibitory effect on this signal transduction pathway. (B, D) The results of semi-quantitative densitometry analysis of the bands from five independent experiments are shown (mean \pm SD); the amount of pERK 1/2 is normalized to that of total ERK 1/2. * $P < 0.05$ vs. vehicle; # $P < 0.05$ vs. VCAM-1.

Figure S6 DS-70 does not induce apoptosis in Jurkat E6.1, EoL-1 and HMC1.1 cell lines. Density plots showing the percentage distribution of Jurkat E6.1, HMC 1.1 and EoL-1 control and vehicle or DS-70 (10^{-4} M; 6 h) treated cells. Apoptotic and necrotic cells were quantified by flow cytometry as described in Methods. Non-apoptotic cells (Annexin V and 7-AAD negative) represent 90–95% of the total cell population after treatment. Quadrants: (top left) damaged cells, (top right) late apoptotic/secondary necrotic cells, (lower left) live cells, (lower right) early apoptotic cells. These figures are from a representative experiment carried out at least five times in triplicate.

Figure S7 Effects of dexamethasone (Dex) on conjunctival symptoms induced by ovalbumin (OVA) in guinea pigs. Guinea pigs sensitized and challenged with ovalbumin and treated with the vehicle used to dissolve DS-70 (vehicle +OVA) were responsive to the treatment with the consequent increase in clinical score index. Administration of Dex significantly counteracts pathological signs and improves eye appearance. In control guinea pigs sensitized with saline and treated with the vehicle (saline+vehicle) or Dex (saline +

Dex 0.1%) no signs of allergic conjunctivitis were observed. Data are presented as scatter plot and refer to the mean \pm SD (5 animals per group were included and both eyes were evaluated; $n = 10$). * $P < 0.05$ vs. saline + vehicle; # $P < 0.05$ vs. vehicle + OVA.

Figure S8 DS-70 prevents, in a dose-dependent manner, conjunctival infiltration and degranulation of mast cells and eosinophils. (A) Histologic analysis of OVA-mediated conjunctival mast cell degranulation. Photomicrographs of tarsal conjunctiva stained with May-Grünwald-Giemsa. Both metachromatic (m) and degranulated (d) mast cells are shown. Black bar = 25 μ m. (B) Substantial eosinophil infiltration (Luna's staining) is observed in OVA-treated guinea pigs (vehicle+OVA) in comparison to animals sensitized with saline and treated with the vehicle used to dissolve DS-70 (saline+vehicle) and to animals sensitized with saline and treated with DS-70 alone (saline+DS-70 0.1%) (5 animals per group were included and both eyes were evaluated; $n = 10$). Scale bar = 100 μ m.

Figure S9 Co-localization of mast cell tryptase or MBP (major basic protein), markers for mast cells and eosinophils respectively, with α_4 integrin in conjunctival sections of guinea pigs sensitized and challenged with ovalbumin and treated with DS-70. (A) Mast cell tryptase and α_4 integrin colocalize on mast cells in conjunctival sections of guinea pig. Double immunofluorescence staining images for tryptase (green) and α_4 integrin (red) are shown. (B) MBP and α_4 integrin colocalize on eosinophils in conjunctival sections of guinea pig. Double immunofluorescence staining images for MBP (green) and α_4 integrin (red) are shown (5 animals per group were included and both eyes were evaluated; $n = 10$). Scale bar = 50 μ m.

Table S1 Primers employed in real time PCR experiments.

Table S2 Cell lines employed in the study; for each cell lines culture medium, integrin mainly expressed and some references are indicated.